THE B&W OWNERS GROUP

Leak-Before-Break Evaluation of Margins Against Full Break for RCS Primary Piping of B&W Designed NSS

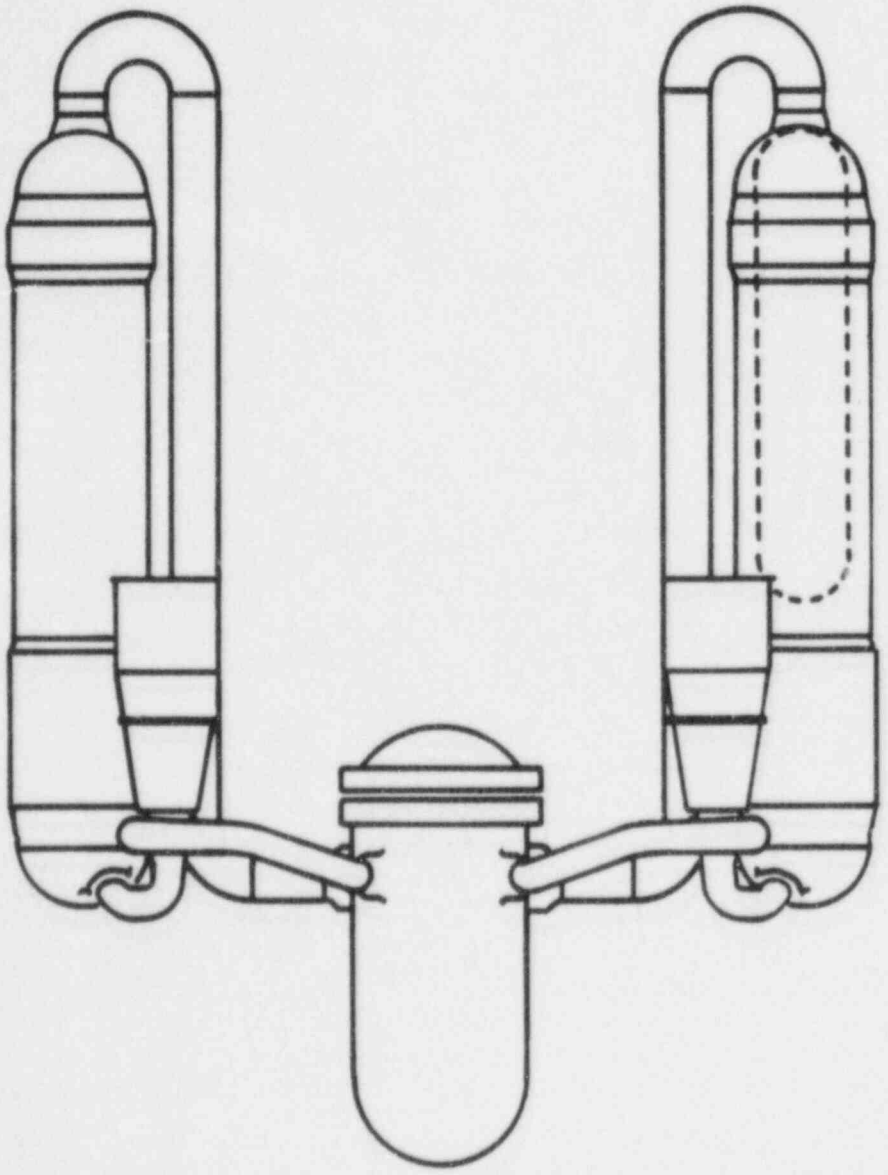

Babcock & Wilcox
a McDermott company

BAW-1847, Rev. 1
77-1153295-01
September 1985

The B&W OWNERS GROUP Leak-Before-Break Evaluation of Margins Against Full Break for RCS Primary Piping of B&W-Designed NSS

Prepared for the
Babcock & Wilcox Owners Group

BABCOCK & WILCOX
Nuclear Power Division
P. O. Box 10935
Lynchburg, Virginia

Babcock & Wilcox
a McDermott company

CONTENTS

CONTENTS (Cont'd)

List of Tables

Tables (Cont'd)

List of Figures

Figures (Cont'd)

1. SUMMARY

One of the many design criteria and requirements for the design of Nuclear Power Plants is referred to in 10CFR50 Appendix A as General Design Criteria 4 (GDC-4). The Nuclear Regulatory Commission's (NRC) interpretation of GDC-4 requires that components such as the reactor vessel (RV) internals, main reactor coolant system (RCS) piping, and piping attached to the RCS piping be able to withstand loads imposed upon them by certain postulated accidents. These accidents include main steam line break (MSLB), operating basis earthquake (OBE), safe shutdown earthquake (SSE), and loss-of-coolant accident (LOCA).

The LOCA definition assumes that the large diameter, thick wall RCS piping ruptures instantly in a guillotine fashion (double-ended guillotine break, DEGB), allowing full flow from both ends of the ruptured pipe. The DEGB requirement historically has been imposed on structures and components even though no known mechanisms could be identified that would cause the piping to fail so catastrophically. As a result, with such large breaks, extremely high forces and moments were determined to exist in the piping, and thus, massive restraints were required to limit pipe whip and the jet impingement of discharged fluid on surrounding components and equipment.

However, both experimental and analytical evidence now exist to show that the main RCS piping could indeed not experience such catastrophic failure, as had been previously postulated. This evidence is presently being applied to a number of pressurized water reactor (PWR) LOCA load issues to solve situations where GDC-4-postulated LOCA loads cannot be tolerated.

Using the leak-before-break (LBB) concept, this report provides the technical basis for evaluating postulated flaw growth in the main RCS piping of B&W-designed NSSs under normal-plus-faulted loading conditions. This evaluation stipulates that a postulated flaw in the RCS piping that might have been missed in inspections during fabrication is smaller than the assumed 10 gpm through-wall leakage flaw shown to exhibit stable growth during the faulted-load application. The LBB evaluation consists of fatigue flaw growth, flaw stability, and limit load analyses to demonstrate that (1) a partial through-wall flaw will propagate in a through-wall direction rather than circumferentially around the pipe, and (2) the RCS piping will remain stable if normal operating plus SSE loads are applied to a postulated leakage flaw within the piping. To obtain the required information the LBB investigation was divided into four technical areas:

- RCS piping structural loads
- Leakage flaw size determination
- RCS piping material properties
- RCS piping fracture mechanics and limit load analyses.

These areas are discussed further in the report.

Thus, this LBB evaluation of the main RCS piping in the B&W Owners' Group (B&WOG) plants has shown that a double-ended guillotine break will not occur and that postulated flaws producing detectable leakage exhibit stable growth, and thus, allow a controlled plant shutdown before any potential exists for catastrophic piping failure.

This revision to the B&WOG LBB Evaluation Report (BAW-1847 Rev. 01) supercedes in its entirety BAW-1847. The report has been revised to include comments made by the NRC staff during their review of the original report. In addition, with the release of NUREG-1061 by the NRC, new methods were suggested for combining axial forces and moments.

Also the B&WOG's materials test program has been completed and now provides material properties for actual materials used in fabrication of the B&WOG piping under a Quality Assured test program.

2. INTRODUCTION AND DISCUSSION

This report has been revised to include suggestions made by the NRC staff during their review of the original leak-before-break (LBB) report submitted to the NRC in October 1984. In addition, NUREG-1061 has been released with additional recommendations. Also the completion of the B&WOG material testing program provided material property data from a Quality Assured test program using actual materials representative of those used in fabrication.

The investigation described in this report evaluates applying the LBB concept to the RCS primary piping of the participating B&WOG plants shown in Table 2-1. The scope of the evaluation includes performing structural and fracture mechanics analyses using generic bounding data (loads and material properties) for all B&WOG plants. The program's objective is to show that sufficient margins to unstable flaw growth and adequate material toughness exist under normal operating loads plus SSE faulted load conditions in the RCS primary piping of the B&WOG plants.

This newly defined faulted load condition of existing operating-plus-dynamic-loads is in contrast to the requirements of Title 10CFR50, Appendix A, GDC-4 that has required that a double-ended guillotine break (DEGB) be postulated as a faulted event and that all of its effects be considered. The interpretation of GDC-4 has evolved to the point that currently the loads from a DEGB must be combined with those from an SSE. This conformance with GDC-4 has resulted in installing large passive restraints, hydraulic snubbers, and jet impingement shields to react to the forces obtained from the assumption of a postulated DEGB at various locations within the RCS piping. However, with the

evidence of successful probabilistic analysis in decoupling DEGB and SSE, and recent developments in fracture mechanics for predicting flaw stability in flawed piping, the DEGB as a design load case can now be eliminated. This has been the topic of discussion among the NRC (Harold Denton), the ACRS, and Atomic Industrial Forum (AIF) over the last two years. Mr. Denton told the AIF in May 1983[1] that the LBB methodology used by Westinghouse and the Lawrence Livermore National Labs (LLNL) probabilistic evaluation are applicable to main loop piping for all PWR systems, including those designed by other NSS vendors. On June 14, 1983 the ACRS stated that "... there is no known mechanism in PWR primary piping material for developing a large break without going through an extended period during which the crack would leak copiously.[2]"

2.1. Effect of GDC-4 Criteria on RCS Designed Loads

General Design Criteria 4 of 10CFR50, Appendix A require that a LOCA be postulated to occur in the RCS primary piping and surrounding structures and components be shielded from the dynamic effects of the LOCA which includes missiles, pipe whip, and jet impingement of the fluid from the break. Thus, the GDC-4 result in design requirements for the major RCS components to withstand large asymmetric loads, jet impingement, and other mechanistic effects. These large forces in turn require massive passive (gapped) restraints and jet shields to prevent pipe whip and protect other systems and components from the postulated breaks.

To meet these conservative design requirements, restraints become massive and costly to build, fabricate, and install. Further, these huge restraints hinder the inservice inspection (ISI) of RCS piping and components throughout the life of the plant. In fact, performing ISI and maintenance of large bore snubbers on the major RCS components requires that some re-

straints in areas of high radiation be dismantled and reinstalled.

The major benefit of applying the LBB concept is eliminating or reducing the need for these cumbersome restraints and thus reducing the exposure of personnel involved in ISI and maintenance. There is also the possibility that normal operating stresses could be higher than expected should the piping contact one of the passive restraints or a hydraulic snubber fail in a locked position. Another potential benefit is that by removing the restraints, the postulated thermal stresses are lower, making a safer plant.

2.2. Application of Leak-Before-Break Concept to Postulated Breaks in the RCS Primary Piping

2.2.1. Leak-Before-Break Concept

The LBB concept has been proposed to justify eliminating the DEGB as a postulated mechanistic event. Relief from this requirement would eliminate the need to design and install costly and massive restraints. The LBB concept is based on a plant's ability to detect an RCS leak and applies known mechanisms for flaw growth to piping designs with assumed through-wall flaws. To ensure adequate margins exist for leak detection, the analysis assumes a leak rate larger than the minimum plant capability.

With various system operating parameters and RCS leak detection capabilities providing the status of the RCS to the operator, a leakage is readily detected and thus an orderly and controlled plant shutdown can be performed before any potential exists for catastrophic pipe failures. Thus, the objective of the application of the LBB concept is to determine that a postulated flaw remains stable under normal operating plus faulted loads or that significant margins exist against unstable flaw growth if the postulated flaw is predicted to grow with the applied loads.

2.2.2. Applicability of Leak-Before-Break Concept to RCS Primary Piping of the B&W NSS Design

This LBB evaluation shows that the LBB condition exists for the RCS primary piping of the B&WOG plants. The investigation shows that (1) any initial flaw tends to grow in the through-wall direction rather than the circumferential or longitudinal direction, and (2) even if any initial flaw should become a through-wall flaw, it will develop sufficient detectable leakage and yet remain stable even under severe loading, including thermal expansion and SSE loads.

Additionally, with the comprehensive requirements for non-destructive pre-service and inservice inspections of the RCS piping, the probability that a through-wall flaw of the size determined to produce 10 gpm leakage is exceedingly small.

Other mechanisms that could cause flaw growth in piping during normal operation are not significant contributors to flaw growth in the RCS primary piping. These contributors are fatigue caused by vibrations, stress-corrosion-cracking, and large forces such as water-hammer in steam and feedwater lines. The B&WOG utilities have operated the B&W-designed NSS for over 53 reactor years spanning some 13 calendar years, without indications of these mechanisms being present to cause degradation of the RCS primary piping. Inservice inspections of RCS primary piping have been completed on various B&WOG plants. The ISI has found no significant flaws or indication of service induced flaws that would result in a reduction of integrity of the RCS piping.

Additionally, the applicability of the LBB concept as discussed in this report focuses on the integrity of the RCS primary piping and does not seek to reduce or re-define GDC-4 LOCA design criteria or qualifications for containment design, release of radioactive materials, and emergency core cooling systems at this time.

Table 2-1. Participating B&WOG Plants Bounded by this Generic LBB Evaluation

Owner	Acronym	Plant
Arkansas Power & Light Co.	AP&L	ANO-1
Consumers Power Co.	CPCo	Midland-2
Duke Power Co.	Duke	Oconee 1, 2, 3
Florida Power Corp.	FPC	Crystal River 3
Sacramento Municipal Utility District	SMUD	Rancho Seco
Supply System	WPSS	WNP-1
Tennessee Valley Authority	TVA	Bellefonte 1, 2
Toledo Edison Co.	TED	Davis-Besse 1

3. LEAK-BEFORE-BREAK EVALUATION OF RCS PRIMARY PIPING

To apply the leak-before-break concept to any piping systems requires various engineering disciplines, computer codes, and various materials properties. In addition, an in-depth evaluation of the assumptions, input data, and methodology used in the LBB analysis must be assessed to maintain a conservative, yet realistic RCS primary piping evaluation.

It is emphasized that strict manufacturing and nondestructive tests were completed on all RCS piping during fabrication by the NSS vendor, thus the piping is not likely to contain any significant size undetected flaws.

3.1. Scope of Investigations for Generic LBB Evaluations

The scope of the B&WOG generic LBB evaluation is to apply the LBB concept to the RCS primary piping, that is the large diameter, high energy piping of the B&WOG plants. This LBB evaluation involves piping made of low alloy-ferritic steels with inner diameters of 28 to 38 inches and varying in thickness from 2.37 to 4.18 inches. The scope includes both 177- and 205-FA plants and configurations of the lowered- and raised-loop design (Figures 3-1 and 3-2). In addition to the piping's ferritic base metals, each weld in the piping, including both shop and field welds, has been represented for the analysis by the material properties obtained from the B&WOG test program.

The only stainless steels involved in B&W designed NSS RCS primary piping are the safe ends welded to the RC pump casings and the casings themselves. The RC pump casings are the only cast stainless within the RCS. In addition the core flood nozzle safe end and piping are stainless steel.

The investigation into the applicability of the LBB concept on the RCS primary piping is divided into four technical areas:

- RCS piping structural loads
- Leakage flaw size determination
- RCS piping material properties
- RCS piping fracture mechanics and limit load analyses.

These areas, as used in the LBB fracture mechanics analysis for the B&WOG are further discussed in the following sections. The flow of information between the various engineering disciplines is illustrated in figure 3-3. The results of the investigations to determine the margins to unstable flaw growth are provided in section 4 and the interpretation of the results are provided in section 5.

The four major areas of investigations that contribute to the final results are outlined here and discussed in detail later in the report.

3.1.1. RCS Piping Structural Loads

The piping loads at various locations on the hot and cold legs of the RCS piping were obtained from existing stress reports for each of the B&WOG plants. These loads, defined in terms of forces and moments, were determined for various thermal loading cases (TH), deadweight (DW), and the applicable SSE loads. The actual combination of these loads (DW + TH + SSE) is discussed in detail in section 3.3.1.

A single set of loads used to determine the generic load set was evaluated for each utility's plant except for CPCo Midland plant, in which two sets of loads were used. These two load sets consisted of the original licensing data and a recently completed reevaluation of the loads on the Midland plant for a snubber optimization study.

3.1.2. Leakage Flaw Size Determination

The leakage flaw size was determined using both loads for internal pressure "only" and for pressure plus the axial and

bending stresses due to minimum operating loads. The leak rate used for determining the leakage flaw size was 10 gpm to provide a margin to the actual plant leakage detection system capabilities designed to meet Regulatory Guide 1.45 requirements of 1 gpm. The initial criterion for the flaw size to be used in the flaw stability analysis was to use the large of either a flaw length of twice the wall thickness (2t) or the 10 gpm flaw length. In each configuration, straight or elbow, and pipe diameter, the 10 gpm flaw size is greater than the 2t flaw. This flaw size determination is discussed further in section 3.3.3.

3.1.3. RCS Piping Material Properties

The initial task was to provide a summary of the materials existing in all the B&WOG plants for both base metal and welds, and then to determine if data for these materials exist, and if it does, is it applicable to the actual materials used in the RCS piping. From the list of the various materials in the RCS piping, it was attempted to collect all material properties that represented a reasonable lower bound. Since there exists insufficient materials data, the B&WOG materials test program was defined in section 3.3.4.4. The newly obtained materials data from this test program was used in this analysis.

All material data used is for non-irradiated materials, since the RCS piping radiation damage is well below the threshold for radiation damage as defined in 10CFR50, Appendix H, paragraph II.A. The materials used in the analysis are discussed further in section 3.3.4.

3.1.4. RCS Piping Fracture Mechanics Analysis

The LBB analysis consists of performing a fatigue flaw growth analysis and elastic and elastic-plastic fracture mechanics analyses. The fatigue flaw growth analysis is performed to show that any postulated small flaws do not grow through-wall during the life of the plant and secondly to define what large size

initial flaw will grow through-wall if it had not been found by either the initial pre-service inspections or by later inservice inspections. The initial flaw size used for fatigue flaw growth analysis is such that the probability of its not being detected is thought to be minimal, if not insignificant.

With a postulated through-wall flaw defined by the leakage flow rate of 10 gpm, a fracture mechanics analysis is performed to establish whether or not this postulated through-wall flaw is stable under existing normal operating loads plus the faulted SSE loads. This provides assurance that sufficient margins to unstable flaw growth remain even with the SSE loads.

In addition to the flaw stability analysis to demonstrate structural stability of the flawed section of the pipe, a limit load analysis was performed to assure adequate margin against the net section failure. The fracture mechanics analysis is discussed further in sections 3.3.2 and 3.3.5.

3.2. LBB Evaluation Criteria

3.2.1. Leak Rate Criteria

To establish the postulated through-wall flaw size for evaluation by the fracture mechanics analysis, a conservative flaw size was determined for various locations throughout the RCS primary piping using a minimum detectable leak rate of 10 gpm for lines with pipe IDs greater than or equal to 28 inches.. The 10 gpm leak rate chosen for the large RCS piping is conservative, since plant leakage detection systems can detect leak rates of 1 gpm as required by B&WOG plant Technical Specifications and Regulatory Guide 1.45. This conservatism provides margins on leakage relative to a plant's leakage detection system capability, by at least a factor of 10.

This method of determining the postulated through-wall flaw size ensures detectability, while providing a conservative input to the fracture mechanics analysis.

3.2.2. Postulated Flaw Size

Initial flaw size is one of the three fundamental data sets needed to perform a fracture mechanics evaluation of a given component. The other two are the existing stress field/loads and material properties.

The flaw selected to demonstrate piping integrity is a circumferentially oriented through-wall flaw. In addition, a longitudinal flaw was considered in the "candy cane" section to represent flaws in the longitudinal seam welds. The through-wall flaw size was selected to ensure detection by normal plant leakage detection systems and provide a conservative model for fracture mechanics analysis. A detectable leak rate of 10 gpm has been used for pipes with inside diameters 28 inches or larger to define the through-wall flaw length. This flaw size is extremely conservative since Technical Specification requirements specify detection of 1 gpm leakage.

As described in section 3.1.2, the leakage flaw size was determined using loads for internal pressure "only" and for pressure plus the axial and bending stresses due to the minimum operating loads. However, the flaw sizes resulting in 10 gpm leakage for the various pipe sizes were obtained using normal operating pressure in combination with the minimum operating loads existing on the piping due to dead weight and thermal expansion. The resulting flaw sizes for the various pipe sizes and minimum operating loads are shown in Table 3-1.

3.2.3. Flaw Stability

Through a tearing instability analysis, the instability point was determined and the applied J integral evaluated for each pipe size with the maximum loads. The results are compared with the J at instability to establish safety margins.

3.2.4. Limit Load Analysis

For each flawed pipe section, a limit moment was calculated and compared with the applied moment based on the 10 gpm through-wall flaw. Then, a series of limit moment calculations were carried out to establish the maximum flaw size with which the limit moment becomes equal to the applied moment. This maximum flaw size (or angle) was compared with the 10 gpm flaw size.

3.3. LBB Investigation Methodology

3.3.1. Determination of Generic Bounding Loads

The loads used in the B&WOG generic LBB analysis are various combinations of deadweight, thermal, and seismic load cases. The load cases were obtained from appropriate plant stress reports and represent a plant's piping system loads at the weld locations under a variety of conditions, such as power level and seismic conditions.

RCS piping load data so defined, in terms of both force and moment vectors, were assembled for the B&WOG plants for the pipe sizes, configurations, load cases, and weld locations specified in Tables 3-2 and 3-3 and Figures 3-5 through 3-10, respectively.

The load at weld locations were sorted twice: first, to obtain a maximum load data set for use in the fracture mechanics analysis; and second, to obtain a minimum load data set for input to the leakage flaw size determination to ensure conservatism.

The initial data sort was performed to determine bounding loads at weld locations for the different pipe sizes and pipe configurations, i.e., straight pipes and elbows. This defines the weld locations of interest for use in the fracture mechanics analysis. This sort allows for a generic analysis, covering all B&WOG plants, while minimizing the number of weld locations that must be considered.

The sorting criterion used to determine the maximum resultant moments is defined by equation 3-1. The criterion is based on existing moments in the piping, since in general, moment is the dominant quantity in defining the state of stress in the large diameter RCS piping.

$$M_{JK} = \left\{ \sum_{I=1}^{3} \left[\left| M_{DW_I} + M_{TH_{I_K}} \right| + \left| M_{SSE_{I_J}} + M_{SSE_{I_Y}} \right| \right]^2 \right\}^{1/2} \qquad (3\text{-}1)$$

where M_{DW} = deadweight moment (signed quantity),
M_{TH} = thermal moment (signed quantity),
M_{SSE} = SSE moment (unsigned quantity),
I = 1(X-direction); =2(Y-direction); =3(Z-direction),
J = X-earthquake or Z-earthquake,
Y = Y-earthquake (vertical direction)
K = 0, 8, 15, or 100% thermal power.

Since a maximum of four thermal load cases (for a given earthquake, X or Z) and two earthquake combinations (X + Y or Z + Y) exist, there is a possibility of eight distinct values of the resultant moment, M_{JK}, being calculated for any given weld location in the RCS piping. Resultant moments were computed for values of J and K, for all weld locations shown in Figures 3-5 through 3-10 and for all B&WOG plants. For a given pipe size and configuration, all values of M_{JK} were then compared with each other. The maximum value of the resultant moment was used to define the bounding weld location for that specific pipe size and configuration for use in the fracture mechanics analysis. The results of this investigation are presented in Table 3-4.

The second data sort was performed to determine a minimal deadweight/thermal loading at weld locations for use in the calculation of flaw length based on axial and bending stresses. The sorting criterion is defined by equation 3-2.

$$M_K = \left\{ \sum_{I=1}^{3} \left[M_{DW_I} + M_{TH_{I_K}} \right]^2 \right\}^{1/2}. \qquad (3\text{-}2)$$

A maximum of four values (corresponding to the four thermal load cases) of M_K were determined for any given weld location. For a given pipe size and configuration, all M_Ks were compared to define the minimum value of the resultant moment, M_K, at the location of interest. Loads at this location were then used to compute an axial pipe stress and a bending pipe stress for input to the leakage flaw length determination described in section 3.3.3. The results of this investigation to define loads for determining leakage flaw length are presented in Table 3-5.

3.3.2. Fatigue Flaw Growth Analysis

Fatigue flaw growth has also been evaluated to demonstrate that postulated surface flaws are likely to propagate in the through-wall direction and develop leakage before they will propagate circumferentially around the pipe. This analysis has been performed based on the linear elastic fracture mechanics and uses the Paris equation provided in Appendix A, Section XI of the ASME Code. This method is applicable to surface flaws that have not fully penetrated the wall.

Longitudinal and circumferential flaws were evaluated, with the BIGIF[3] code, using the stresses and cycles for the ASME Code transient fatigue analysis plus the SSE loadings. Results of these analyses are discussed in section 4.3 and support the assumption that cracks progress radially through the wall and result in leak-before-break conditions.

The RCS primary piping is designed, fabricated, and inspected in accordance with the requirements of the ASME Section III Code, which requires that indications longer than three inches and deeper than 10% of the pipe wall thickness be removed. From the fatigue flaw growth analysis, the flaw sizes that grow through-wall are clearly many times those allowed by the Code and represent a very conservative estimate of any existing flaws.

3.3.3. Determination of Leak Rate Flaw Size

The relationship between flaw length and the flow rate through the flaw was established using the B&W computer code, KRAKFLO.[4] This code's heritage resides in work performed by Battelle Columbus Laboratories and the Electric Power Research Institute. KRAKFLO is similar to the NRC's code, LKRATE.[5] KRAKFLO's flaw geometry is based on NUREG/CR-3464[6] and its flow rate calculation on NUREG/CR-1319[7] and EPRI-NP-3395.[8]

KRAKFLO calculates the two-phase flow through the flaw considering system pressure, temperature, and flow rate, flaw surface roughness, pressure differential across the flaw, flaw length, pipe diameter and wall thickness, and flaw area resulting from applied pipe loads. KRAKFLO was benchmarked against the Battelle Columbus Laboratories data as presented in EPRI-NP-3395 (Tables 2-1 and 2-2). The predictions of leak rate using KRAKFLO agreed well with the experimental data.

Flaw length and leakage calculations were based on the pipe dimensions, thermodynamic properties, and material properties presented in Table 3-6; pipe cladding was not considered in the leakage calculations. Material properties were taken from the 1983 ASME Code at 600F. The system parameters of 2150 psi and 600F used in this analysis represent realistic values, existing in the B&WOG plants during normal full-power operation. If the system parameters vary significantly from these conditions, operators will be alerted by various alarms, such as low RCS pressure and low makeup tank or pressurizer level. Additionally, 2150 psi and 600F compare closely (1-2%) to the worst plant pressure and temperature conditions for normal operations, i.e., hydraulically, as RCS pressure goes down leak flow goes down and as RCS temperature goes up leak flow again goes down.

Using KRAKFLO, postulated through-wall flaw lengths were established for pipe sizes of inner diameters of 28 to 38 inches. These flaws correspond to an assumed leak flow rate of 10 gpm. All calculations were based on a flaw surface roughness of 5 μm.

3.3.4. RCS Primary Piping Materials Data

3.3.4.1. Materials Used in the Manufacture of 177-FA and 205-FA B&W-Designed NSS Systems

The subassembly drawings and construction records of the RCS primary piping for the Consumers Power Midland plants were examined to tabulate the materials in the RCS primary piping, including individual sections of piping and elbows, nozzles, and weldments. The as-built drawings and materials lists for all B&WOG plants were reviewed and a complete materials list assembled, including possible weld metal combinations. The system materials are predominantly low-allow ferritic steels, with some stainless steel and Inconel in the vicinity of the reactor coolant pumps and core flood nozzles. The RCS primary piping materials list is shown in Table 3-7, with possible weld metal combinations shown in Table 3-8. A schematic layout showing the locations of the various materials in a typical B&W-designed NSS system is shown in Figure 3-11.

3.3.4.2. Review of Available Materials Data for Use in RCS Piping Evaluation

A list of representative materials, consisting of materials considered to encompass the RCS piping materials in Figure 3-11, was compiled (Table 3-9). The RCS primary piping would be completely defined if all twelve material properties existed.

The existing data pertinent to the representative materials matrix were reviewed; sources of data included B&W's Alliance Research Center, Materials Engineering Associates, David Taylor Naval Ship R&D Center, literature, and file reports. True stress-true strain data and full J_I-R curves were needed for each material. Data had to be in the 540-610F temperature range, with the material in a condition similar to that of the material in the RCS primary piping. Table 3-10 is a summary of the type of data found during this review. This data was then compared with the data needed, as shown in Table 3-11. As can

be seen, only one weld metal met all the above requirements as well as the NRC criterion for three heats of a material. This result led to a B&WOG LBB Task Force decision to test several materials for comparison with data found in the literature. This data is now available (ref. 17) and has been used in this analysis.

3.3.4.3. Review of Material Properties Thermal Stability (Aging Sensitivity)

Since the ferrite steels used in fabricating the RCS piping of B&W designed NSS are the same as those used for fabricating fossil boilers, a large amount of thermal exposure data at temperatures well above those of the RCS piping have been obtained. This operating experience has demonstrated the reliability of these materials at conditions that should demonstrate the effects of thermal aging if present. When failures of these materials have occurred analysis has shown the failures to be from poor processing and/or poor design. In these cases, metallurgical stability has been retained. Thus, the evaluation of the RCS piping materials for thermal aged condition does not appear necessary since it is expected that the materials properties used in the LBB evaluation will encompass the material properties for aged material.

The austenitic stainless steels in the RCS piping are in two forms - wrought and cast. The wrought stainless steels have demonstrated good thermal stability during service at conditions similar to those experienced in the RCS. The cast austenitic stainless steels, because of their metallurgical composition have shown a sensitivity to thermal aging. The degradation in fracture toughness properties reported for the cast stainless materials is large relative to their initial values, but the aged condition values are acceptable for these LBB analyses. The reported values for aged cast stainless steel are encompassed by the values selected for this evaluation as representative design values.

Based on the above information and the representative material properties in this analysis, it is believed unnecessary to further consider the effects of thermal aging on material properties of RCS piping materials. Since these materials are widely used in similar elevated temperature applications, further information and service experience on the effects of thermal aging will become available.

3.3.4.4. Materials Testing to Support LBB Evaluation

Based on the findings detailed in section 3.3.4.2 a test program was defined to provide material data for use in the LBB Evaluation. The material test program was conducted at the B&W Alliance Research Center. The test results are documented in reference 17. The material test matrix is shown in Table 3-12. The test program provided a quality assured data base for low-alloy ferritic steels and weldments in the appropriate heat treatment conditions representative of those received by the actual operating hardware. Two sets of bounding material data were chosen for the LBB analysis described in section 4.4. The two sets of data represent both the weld and base metals used in fabrication of the RCS piping in the B&WOG plants.

3.3.5. Flaw Stability Analysis

Considering the operating temperature range and the materials used for fabricating the RCS piping of the B&WOG plants, fracture mechanics analyses of the flawed piping are in the ductile tearing region. Therefore, the first step in the LBB evaluation is to determine whether or not the postulated through-wall flaws will begin to tear in a stable manner, and secondly, if they do, determine how far the flaws will tear before they become unstable. The critical stress intensity factor or its equivalent at the initiation of ductile tearing will be used to determine if flaw initiation occurs and a tearing stability evaluation will be used to address the instability question.

3.3.5.1. Stress Intensity Factor Evaluation

To ensure the adequacy of the methodology, the results of the Paris-Tada equations[6] and the finite element program MARC[9] were compared. The MARC code was used due to its capability to model the pipe elbow sections.

The stress intensity factors given in reference 6 are as follows:

$$K_p = \sigma_A \sqrt{\pi R \theta}\, F_p(\lambda)$$

$$K_t = \sigma_t \sqrt{\pi R \theta}\, F_t(\theta)$$

$$K_b = \sigma_b \sqrt{\pi R \theta}\, F_b(\theta)$$

where σ_A, σ_t and σ_b are stresses due to end cap pressure, tension and bending; R is mean radius; and, θ is one half of the flaw angle for a through-wall flaw (see Figure 3-12) and $F_p(\lambda)$, $F_t(\theta)$ and $F_b(\theta)$ are non-dimensional functions determined by the following approximate expressions representing the numerical values calculated for R/t=10.

$$F_p(\lambda) = (1 + .3225\,\lambda^2)^{1/2} \qquad (0 \le \lambda \le 1)$$

$$= .9 + .25\lambda \qquad (1 \le \lambda \le 5)$$

where $\lambda = \dfrac{R\theta}{\sqrt{Rt}}$

$$F_t(\theta) = 1 + 7.5\left(\frac{\theta}{\pi}\right)^{3/2} - 15\left(\frac{\theta}{\pi}\right)^{5/2} + 33\left(\frac{\theta}{\pi}\right)^{7/2}$$

$$F_b(\theta) = 1 + 6.8\left(\frac{\theta}{\pi}\right)^{3/2} - 13.6\left(\frac{\theta}{\pi}\right)^{5/2} + 20\left(\frac{\theta}{\pi}\right)^{7/2}$$

$$(0 < \theta < 100^{o}).$$

When the pipe is subjected to an axial force, internal pressure and bending moment at the same time, the total stress intensity factor is obtained by superposition of the separate factors, i.e.

$$K_{total} = K_t + K_b + K_p.$$

These equations are valid for a straight section of pipe.

Since the "candy cane" section in the hot leg of the RCS primary piping in the B&WOG plants consists of a 180° double elbow, a finite element method computer program was used to model this elbow section. The finite element program, MARC, utilizes the isoparametric shell elements with quarter point nodes and has been used before for this type of application.[10] Validation of this approach was documented in reference 11; independent verifications were made by comparing the MARC analysis with selected calculations by the Paris-Tada equation.

MARC utilizes Park's virtual displacement method[12] which has been demonstrated to produce accurate results without the need for special flaw tip elements. The finite element models of a quarter section of the elbows are shown unrolled in Figures 3-13 and 3-14 for the straight pipe sections and are rolled into the configuration for the hot leg elbow shown in figure 3-15. These models were made from the eight noded isoparametric shell elements and along the flaw tip the quarter point modeling technique was used to achieve flaw tip singularity. The models used are quarter sections, taking advantage of symmetry about the longitudinal and circumferential axes. The boundary remote from the flaw is permitted to move axially and rotate as a plane. The forces on the boundary are the resultant shears and moments which induce a tensile stress field around the flaw tip.

For the B&W Owners Group plants the RCS piping is grouped by size and maximum applied loads. Linear Elastic Fracture Mechanics (LEFM) analyses were performed on all pipe sections with the results compared to the fracture toughness of the controlling material. If the applied K_I exceeds the material toughness K_{IC} further analysis using elastic plastic fracture mechanics (EPFM) is required. If the applied K_I is less than K_{IC}, there is no flaw initiation from the existing flaw under the applied loads.

3.3.5.2. Evaluation of Tearing Instability

The EPFM analysis is based on the J integral[13] which is a measure of flaw driving force in both elastic and elastic plastic range. In the elastic range, J can be directly related to the stress intensity factor K_I. This applied J is to be evaluated against the J_I-R curve which is a material property obtained from compact tension specimen tests.

To ensure the adequacy of the analytical techniques, two methods were used for the evaluation of the J-integral in the elastic-plastic domain. The methods are the MARC finite element code and the EPRI/GE estimation method.[14] The finite element models generated for the linear elastic analyses were also used in the EPFM, with multiple iteration and scale loading options. As noted in section 3.3.4.1, the B&W designed RCS is fabricated from ferritic materials which exhibit substantial strain hardening behavior. The two methods used in this analysis take into account strain hardening. The EPRI/GE method uses a Ramberg-Osgood representation of the material stress-strain relationship and the MARC code accepts a number of stress-strain values as input to include the strain hardening behavior of the material.

The flaw instability point can be determined by the J-T method described in reference 15 where T is the tearing modulus defined as,

$$T = \frac{E}{\sigma_o^2} \frac{dJ}{da} \qquad (3\text{-}5)$$

where E is Young's modulus and σ_o is the flow stress. The tearing modulus is a dimensionless parameter.

The condition for stable crack is that the material's tearing modulus is greater than the tearing modulus obtained from the applied loads. That is, where:

$$T_{applied} < T_{material} \qquad (3\text{-}6)$$

Evaluation of tearing instability can be illustrated by a plot showing J versus T as shown in Figure 3-16. The intersection point of the two curves is the instability point and the corresponding J value is designated as $J_{instability}$ from which a critical load value can be evaluated. A safety factor on load is thus defined as the ratio between the critical load and the applied load.

The EPRI/GE method for J integral for through-wall flaws under bending moment M is:

$$J = f_1\left(a_e, \frac{R}{t}\right)\frac{M^2}{E} + \alpha\,\sigma_o\,\varepsilon_o\,c\,\frac{a}{b}\,h_1\left(\frac{a}{b}, n, \frac{R}{t}\right)\left[\frac{M}{M_o}\right]^{n+1} \qquad (3\text{-}7)$$

where

$$c = R(\pi - \theta)$$

$$a = R\theta$$

$$b = R\pi$$

$$f_1\left(\frac{a}{b}, \frac{R}{t}\right) = \pi a\left(\frac{R}{I}\right)^2 F^2\left(\frac{a}{b}, \frac{R}{T}\right)$$

$$M_o = M_o'\left[\cos\left(\frac{\theta}{2}\right) - \frac{1}{2}\sin(\theta)\right] .$$

$$M_o' = 4\sigma_o R^2 t$$

M_o' is the limit moment of an uncracked cylinder and σ_o here is the yield stress, not the flow stress of the material. The parameters F and h_1 are dependent on the flaw ratio and the Ramberg-Osgood material constants α and n. The F and h_1 values were obtained by a series of deformation plasticity finite element analyses and tabulated in the EPRI/GE method.

3.3.6. Limit Load Analysis

The original RCS piping design analysis included a net section plastic collapse analysis to show that a non-flawed pipe section would not fail by an instability due to the limit load. In the LBB evaluation, pipes with postulated through-wall flaws are subjected to various loadings, therefore it is prudent to

demonstrate that the pipe sections with postulated through-wall flaws will not fail due to plastic instability.

For the LBB analysis the following limit moment, Mp, relations of Paris and Tada for flawed pipe sections (reference 6) were used;

$$M_p = \sigma_o (4R^2 t) \bar{M}_p$$

where
$$\bar{M}_p = (1 - \bar{a}) \left(\cos \alpha - \frac{1}{2} \sin \theta\right) \qquad (3\text{-}8)$$
and

$$\alpha = \frac{1}{2}\theta + \frac{\pi}{2} \frac{\bar{P}}{1 - \bar{a}}$$

$$\bar{P} = \left[\left(\frac{P}{2\pi Rt}\right) + \left(\frac{pR}{2t}\right)\right] / \sigma_o$$

$$\bar{a} = a/t$$

P = axial force (kips)
R = mean pipe radius (in.)
t = pipe wall thickness (in.)
p = internal pressure (ksi)
σ_o = flow stress (ksi)
a = depth of part-through circumferential flaw
t = pipe thickness

Table 3-1. Leakage Flaw Sizes for Various RCS Pipes

Pipe ID, in.	Minimum moment, ft-kips	Internal pressure, psi	Flaw length (pressure & min. loads), in.
38S	2407	2150	9.0
	991	2150	10.4
38E	916	2150	12.3
	1890	2150	12.0
36S	2284	2150	8.0
	1010	2150	9.8
36E	1010	2150	10.8
32S	1159	2150	9.2
32E	1122	2150	10.6
28S	560	2150	9.2
	1095	2150	7.9
	1246	2150	7.7
28E	1246	2150	9.0
	871	2150	9.6
	1278	2150	9.0

S = straight section of pipe.

E = elbow section of pipe.

Table 3-2. Reactor Coolant System Pipe Sizes Evaluated in the Leak-Before-Break Fracture Mechanics Analysis

Plant category	Pipe, ID, in.
205-FA (nozzle supported)	38, 32, 28, and 11.5
177-FA raised loop (nozzle supported)	36, 28, and 11.5
177-FA low loop (skirt supported)	36, 28, and 11.5

Table 3-3. Load Cases Evaluated for Determining Input to the Fracture Mechanics Analysis

Plant	Load cases
Bellefonte 1,2	DW; 0,8,15, and 100% (power) thermals; OBE; SSE
WNP-1	DW; 0,8,15, and 100% thermals; OBE; SSE
Davis-Besse 1	DW; 8,15, and 100% thermals; OBE; SSE (2 x OBE)
Oconee 1,2,3	DW; 15 and 100% thermals; OBE; SSE (2 x OBE)
Crystal River 3	DW; 15 and 100% thermals; OBE; SSE (2 x OBE)
ANO-1	DW; 8,15, and 100% thermals; OBE; SSE (2 x OBE)
Rancho Seco	DW; 8,15, and 100% thermals; OBE; SSE (2 x OBE)
Midland-2	DW; 0,8,15, and 100% thermals; OBE; SSE (2 x OBE)
Midland-2 (SR)	DW; 0 and 15% thermals; OBE; SSE (2 x OBE)

- - - - -

DW -- deadweight

2 x OBE -- SSE loads are taken as being twice the OBE loads

SR -- snubber removal study results

Table 3-4. Bounding Weld Locations for Input to the Fracture Mechanics Analysis

Pipe ID, in.	Pipe configuration	Plant	Weld location Number[1]	Weld location Description
38 nozzle	Straight	Bellefonte	15	RV outlet
	Elbow	Bellefonte	2	Exit HL 180° elbow
36 nozzle	Straight	Davis-Besse 1	15	RV outlet
	Elbow	Oconee 1,2,3	13	Exit HL 90° elbow
32	Straight	Bellefonte	305	Pump suction nozzle
	Elbow	WNP-1	301	Once-through steam generator outlet nozzle
28	Straight	Oconee 1,2,3	12	RV inlet nozzle
	Elbow	Oconee 1,2,3	24	Exit LCL 90° elbow

[1]Refers to the numbering scheme on Figures 3-5 through 3-10.

Table 3-5. Minimum Loads at Weld Locations Used to Determine Leakage Flaw Size

Pipe ID, in.	Pipe configuration	Plant	Weld location Number[1]	Weld location Description
38	Straight	WNP-1	8	HL vertical run
	Elbow	WNP-1	3	Mid-point 180° elbow
36	Straight	Midland	7	HL vertical run
	Elbow	Davis-Besse 1	3	Mid-point 180° elbow
32	Straight	WNP-1	205[2]	Pump suction nozzle
	Elbow	WNP-1	204[2]	Exit LCL 90° elbow
28	Straight	ANO-1	15.5[3]	Exit UCL middle elbow
	Elbow	ANO-1	15.5[3]	Exit UCL middle elbow

[1]Refers to the numbering scheme on Figures 3-5 through 3-10.

[2]205 and 204 are the same weld location as 305 and 304 respectively, except that they are on the lower cold leg (LCL) in the negative X-direction (-X +Z quadrant).

[3]15.5 is the same weld location as 15, except that it is on the upper cold leg (UCL) in the negative X-direction (-X +Z quadrant).

Table 3-6. Flaw Length and Leakage Calculational Input Properties

Pipe ID, in.	Unclad ID, in.	Thickness, in.	Material	Yield, psi	Young's Modulus, psi
38 straight	38.5	3.125	SA-106, GR C	29,600	26.5E+6
38 elbow	38.5	4.1875	SA-516, GR 70	28,100	26.5E+6
36 straight	36.5	2.9375	SA-106, GR C	29,600	26.5E+6
36 elbow	36.5	3.75	SA-516, GR C	28,100	26.5E+6
32 straight	32.5	2.6875	SA-106, GR C	29,600	26.5E+6
32 elbow	32.5	3.625	SA-516, GR 70	28,100	26.5E+6
28 straight	28.5	2.375	SA-106, GR C	29,600	26.5E+6
28 elbow	28.5	3.125	SA-516, GR 70	28,100	26.5E+6

System pressure: 2150 psi
System temperature: 600F
} Generic values

Table 3-7. RCS Primary Piping Materials List

BASE METAL

1. SA508 C1.1 (OTSG nozzles -- 177-FA)
2. SA508 C1.2 (all RV nozzles; OTSG nozzles -- 205-FA)
3. SA106 GR. C (seamless pipe)
4. SA516 GR. 70 (pipe elbows)
5. SA376 TP316 (seamless pipe)
6. SA351 CF8M casting (RC pump casing)
7. SA336 (65) F8m (core flood nozzle safe ends -- 177-FA)
8. SB166 (core flood nozzle safe ends -- 205-FA)

WELD FILLER METAL

1. HiMnMo (SMA[1] process)
2. MnMoNi (SMA process)
3. E308 (SMA or GTA[2] process)
4. E309 (SMA or GTA process)
5. E316 (SMA or GTA process)
6. E182 (MMA[3] process)
7. E7015 (MMA process)
8. E8018 (MMA process)
9. E8015 (MMA process)
10. E8018 (MMA process)

[1]SMA -- automatic submerged metal arc weld process. All carbon steel SMA welds may have used wither MnMoNi or HiMnMo filler metal.

[2]GTA -- tungsten electrode, inert gas weld process.

[3]MMA -- manual metal arc (stick) weld process. All carbon steel MMA welds may have used E7015, E7018, E8015, or E8018 filler metal.

Table 3-8. Possible RCS Primary Piping Weld Metal Combinations

Weld filler	Base metal combinations: SA508 Cl.2 buttering	SA106C buttering	SA516-70 buttering	HiMnMo/ MnMoNi buttering SA106C	SA376 TP316 to Inconel 182 buttering	SA336F8m to Inconel 182 buttering	SA106C to SA516-70	SA516-70 to SA516-70	SA106C to SA106C	SA106C to SA508 Cl.1 or Cl.2	SA376 TP316 to SA351 CF8M	SB166 to Inconel 182 buttering
Shop												
HiMnMo	X						X	X	X			
MnMoNi	X						X	X	X			
E7015							X	X	X			
E7018							X	X	X			
E8015							X	X	X			
E8018							X	X	X			
Inconel 182	X	X	X		X	X						X
Field												
E7015				X						X		
E7018				X						X		
E8015				X						X		
E8018				X						X		
E308											X	
E309											X	
E316											X	

Table 3-9. Representative Materials Matrix

1. SA508 Cl.1 -- covers SA 508 Cl.1 and Cl.2
2. SA106C
3. SA516-70
4. SA376 TP316 -- covers SA376 TP316 and SA336 (65) F8m
5. SA351 CF8M
6. SB166
7. SMA weld, SA106C to SA516-70, HiMnMo filler -- covers all HiMnMo welds and buttering.
8. SMA weld, SA516-70 to SA516-70, MnMoNi filler -- covers all MnMoNi welds and buttering.
9. MMA weld, SA206C to SA106C, E8015 filler -- covers all E8015 and E8018 welds.
10. MMA weld, SA106C to SA508 Cl. 1, E7018 filler -- covers all E7015 and E7018.
11. MMA weld, SA376 TP316 to SA351 CF8M, E308 filler -- covers all E308, E309, E316 welds.
12. SMA weld, SA376 to SB166, Inconel 182 filler -- covers all Inconel welds and buttering.

Table 3-10. Summary of Available Materials Data Related to LBB Analysis

Material	Type	Lower bound J_{IC} in.-lb/in.^{2}	True $\sigma - \varepsilon$ curves	QA	Source
SA106,Cl.C	BM	468	Yes	No	B&W
SA516,Gr.70	BM	252	No	No	B&W[1]
Type 304	BM	4012	Yes	?	W[3]
Type 316	BM	3849	No	?	W
CF8A	BM	No	No	No	--
MnMoNi	WM(SA)	404	Yes	Yes	B&W
Type 304	WM(SA)	556	Yes	?	W
	WM(TIG)	930	Yes	?	W
	WM(MA)	990	No	?	W
Type 316	WM(MA)	930	No	?	W
CF8A	WM	507	No	No	DTNSRDC[2]

[1]J-K multi-specimen technique.

[2]David Taylor Naval Ship Research Development Center.

[3]Westinghouse data.

All data shown in the temperature range of interest.

BM = base metal
BM(SA) = weld metal submerged arc.
WM(SA) = weld metal manual arc.
WM(TIG) = weld metal tungsten inert gas

Table 3-11. A Comparison of Materials Data Available for Those Materials Included in the Representative Materials Matrix

Material	Type	J-R data	True σ-ε data	QA	Three heats
SA508, Cl.1	BM	No	No	No	No
SA106C	BM	Yes	Yes	No	No
SA516-70	BM	Yes	No	No	No
SA376 TP316	BM	Yes	No	?	No
SA351 CF8M	BM	No	No	No	No
SB166	BM	No	No	No	No
Subarc weld HiMnMo	Weld	No	No	No	No
Subarc weld MnMoNi	Weld	Yes	Yes	Yes	Yes
Manual weld E801X	Weld	No	No	No	No
Manual weld E701X	Weld	No	No	No	No
Manual weld E308	Weld	No	No	No	No
Subarc weld Inconel 82	Weld	No	No	No	No

Table 3-12. Materials Test Program in Support of the LBB Evaluation of the RCS Primary Piping

Materials	Specimens			
	Heats	CV[2]	Tensile[1]	Compacts[1,3]
Base Metals				
SA 106C	1	12	2	2
SA 516 70	1	12	2	2
SA 508 Cl. 1	1	12	2	2
Weld Metals				
SMA HiMnMo	3	36	6	6
MMA EX015/X018	3	36	6	6

[1]Test at one temp 550F.

[2]Tested for full curve.

[3]2T compact specimens.

Figure 3-1. Typical Lowered Loop Reactor Coolant System Arrangement - Elevation

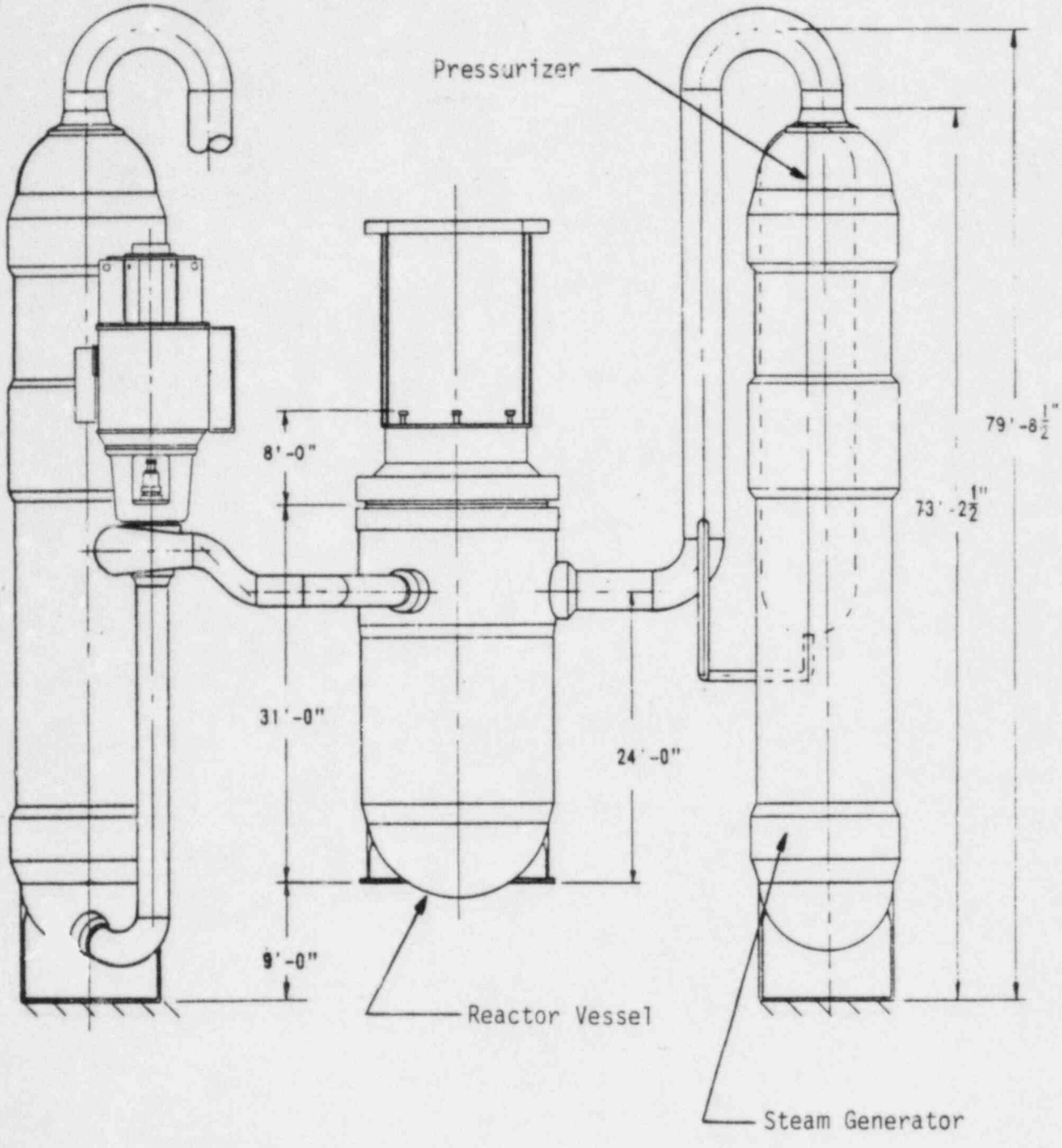

Figure 3-2. Typical Raised Loop Reactor Coolant System Arrangement - Elevation

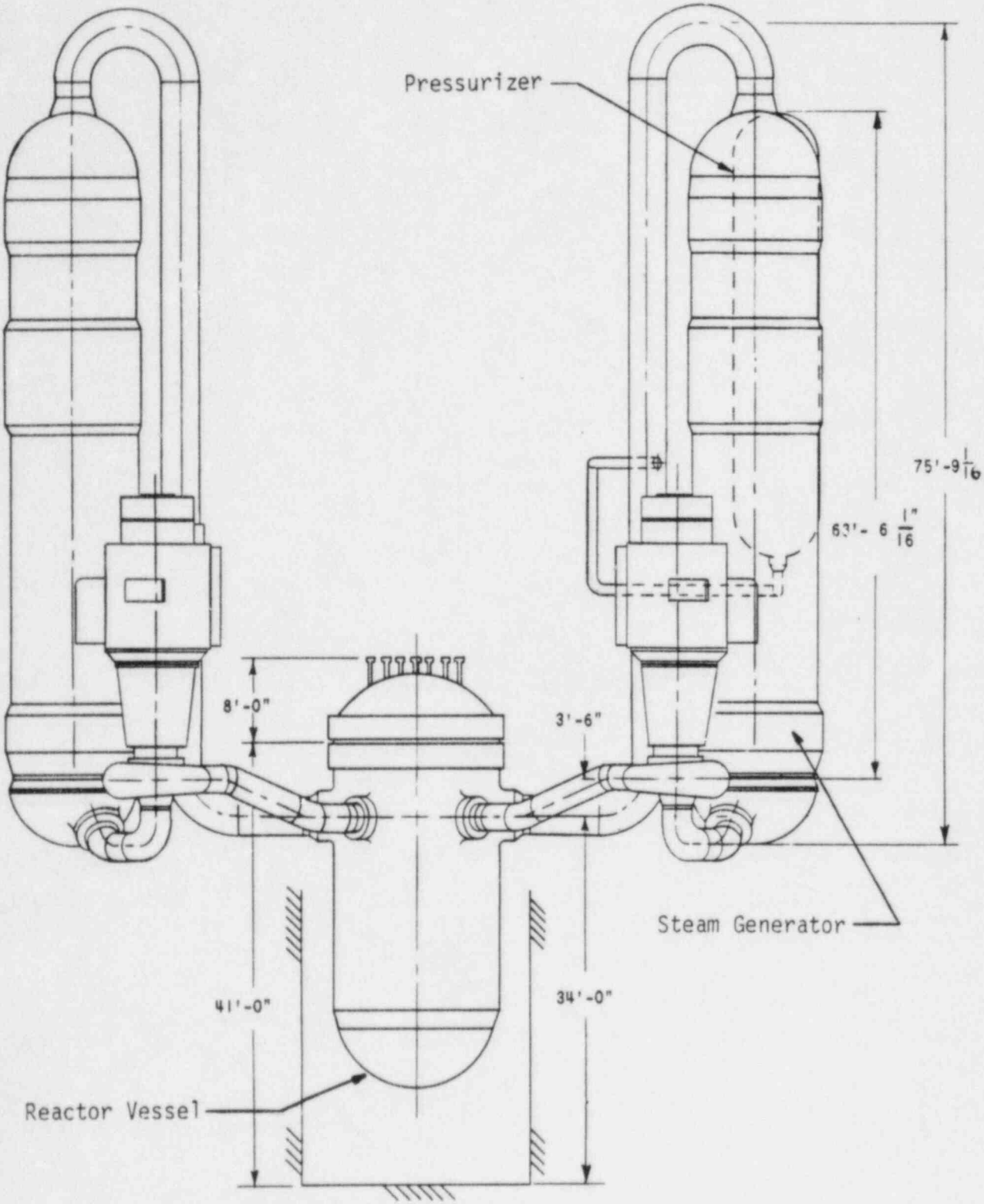

Figure 3-3. Leak-Before-Break Investigation for RCS Primary Piping

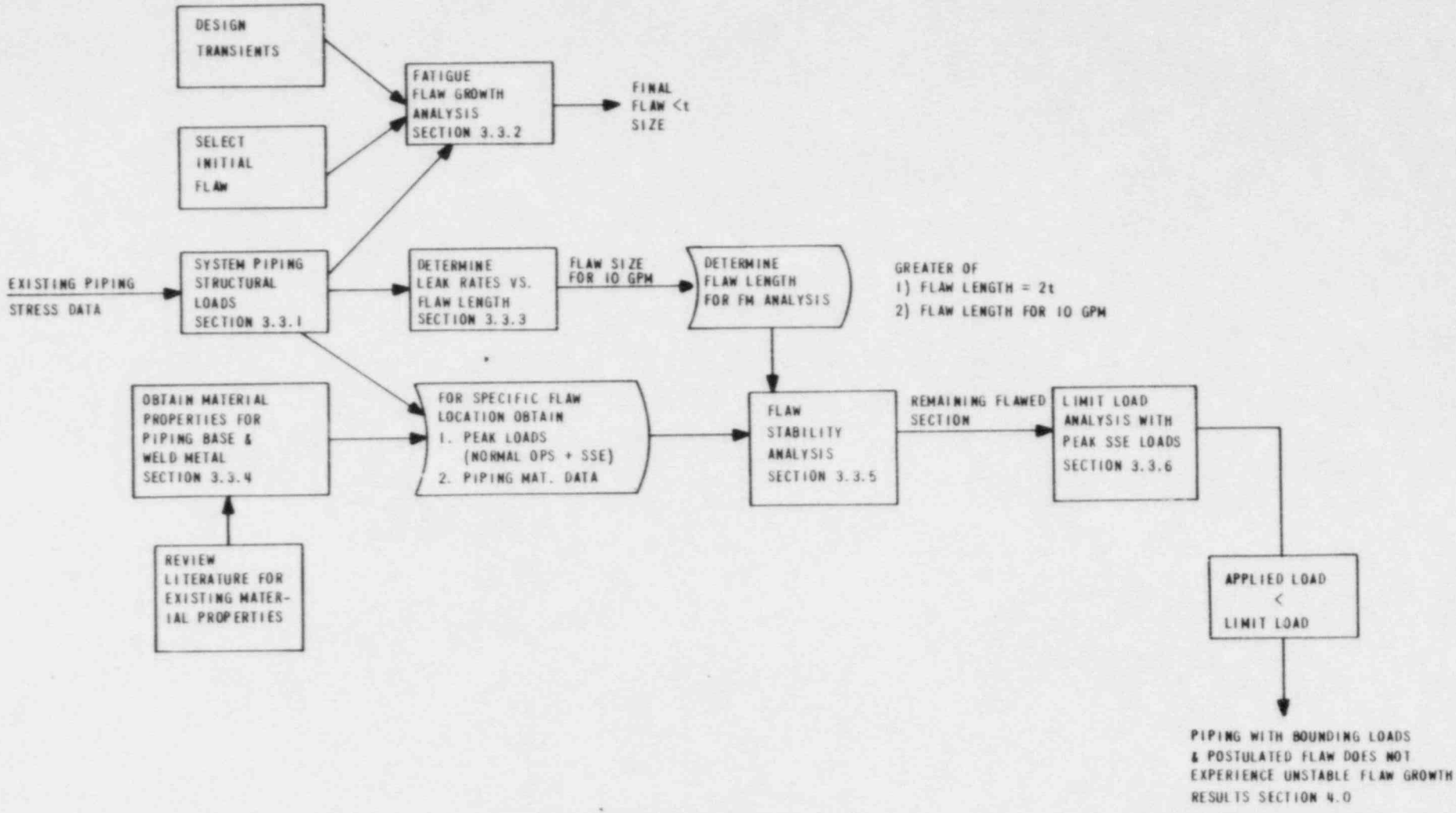

This page intentionally left blank

Figure 3-5. 205-FA Plant Hot Leg Weld Locations

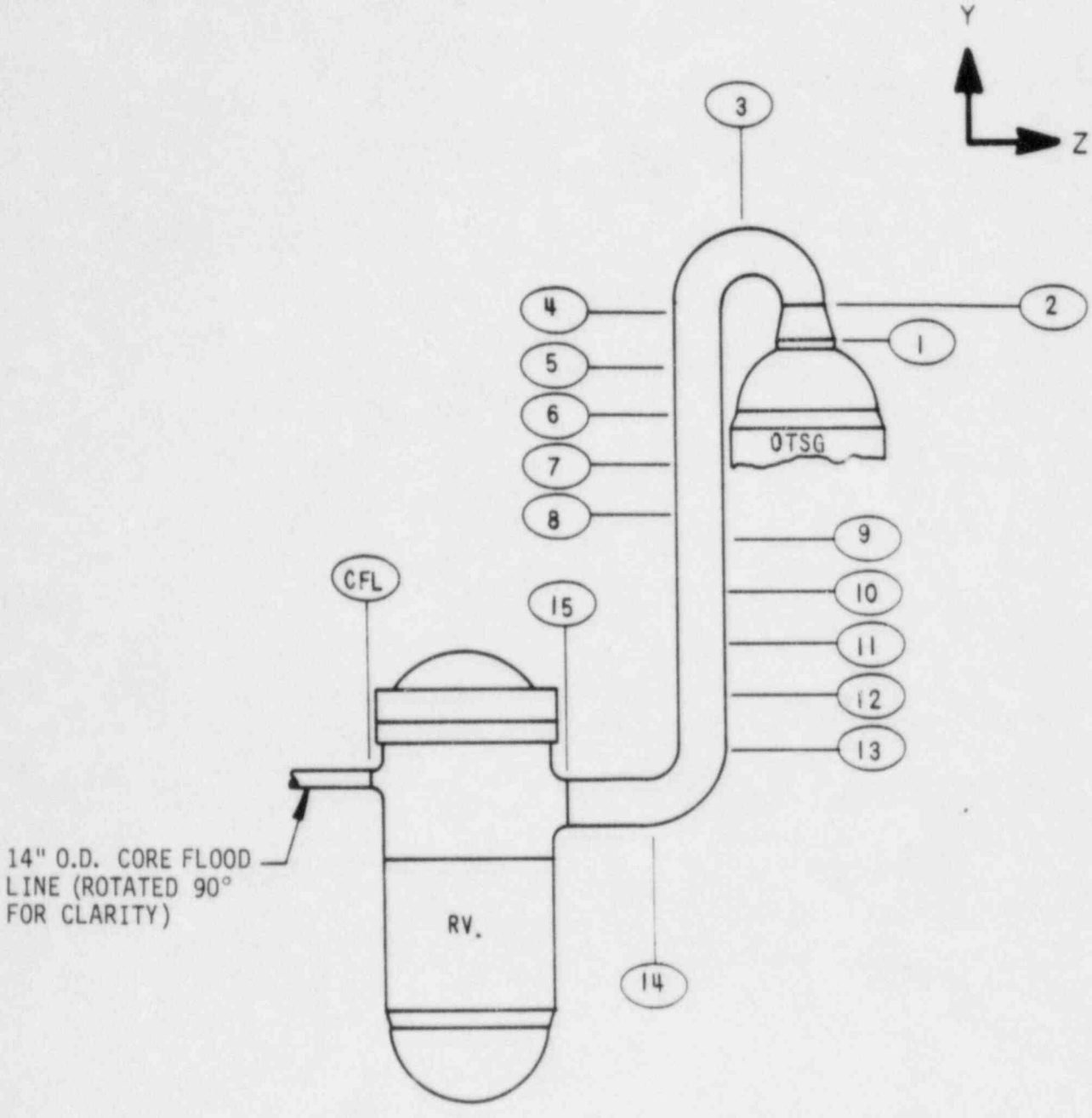

Figure 3-6. 205-FA Plant Cold Leg Weld Locations

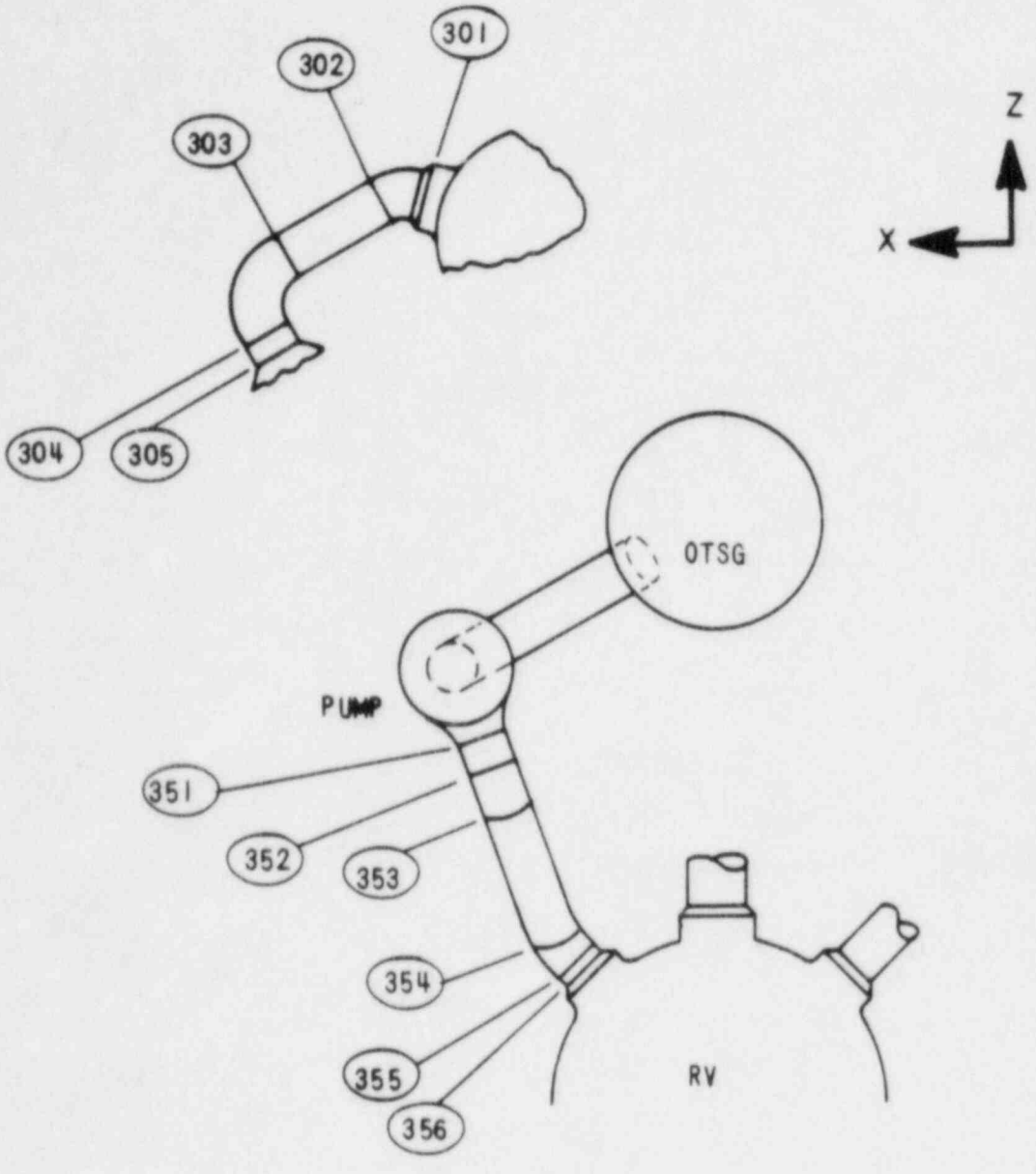

Figure 3-7. 177-FA Plant Raised Loop Weld Locations

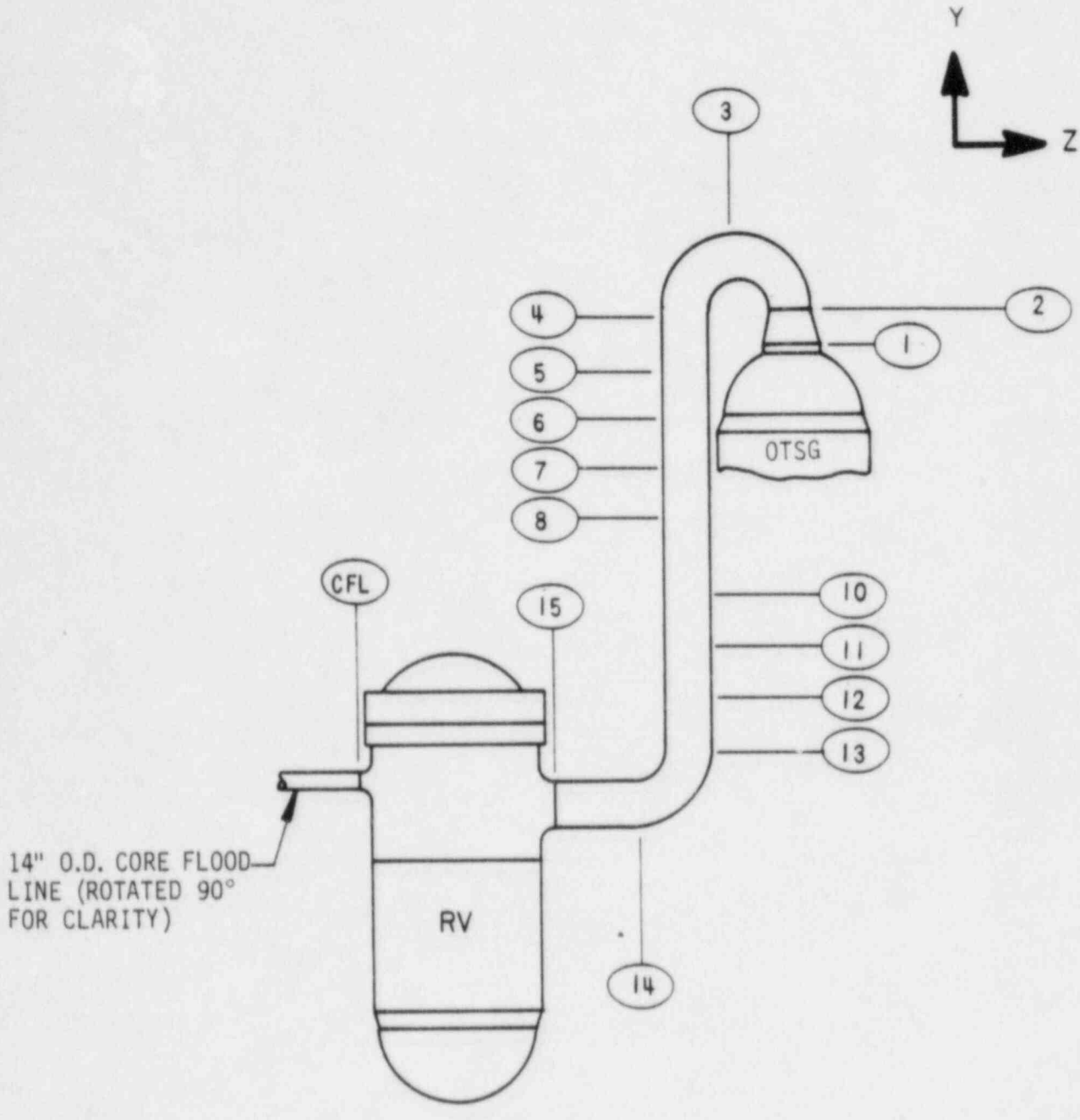

Figure 3-8. 177-FA Plant Raised Loop Cold Leg Weld Locations

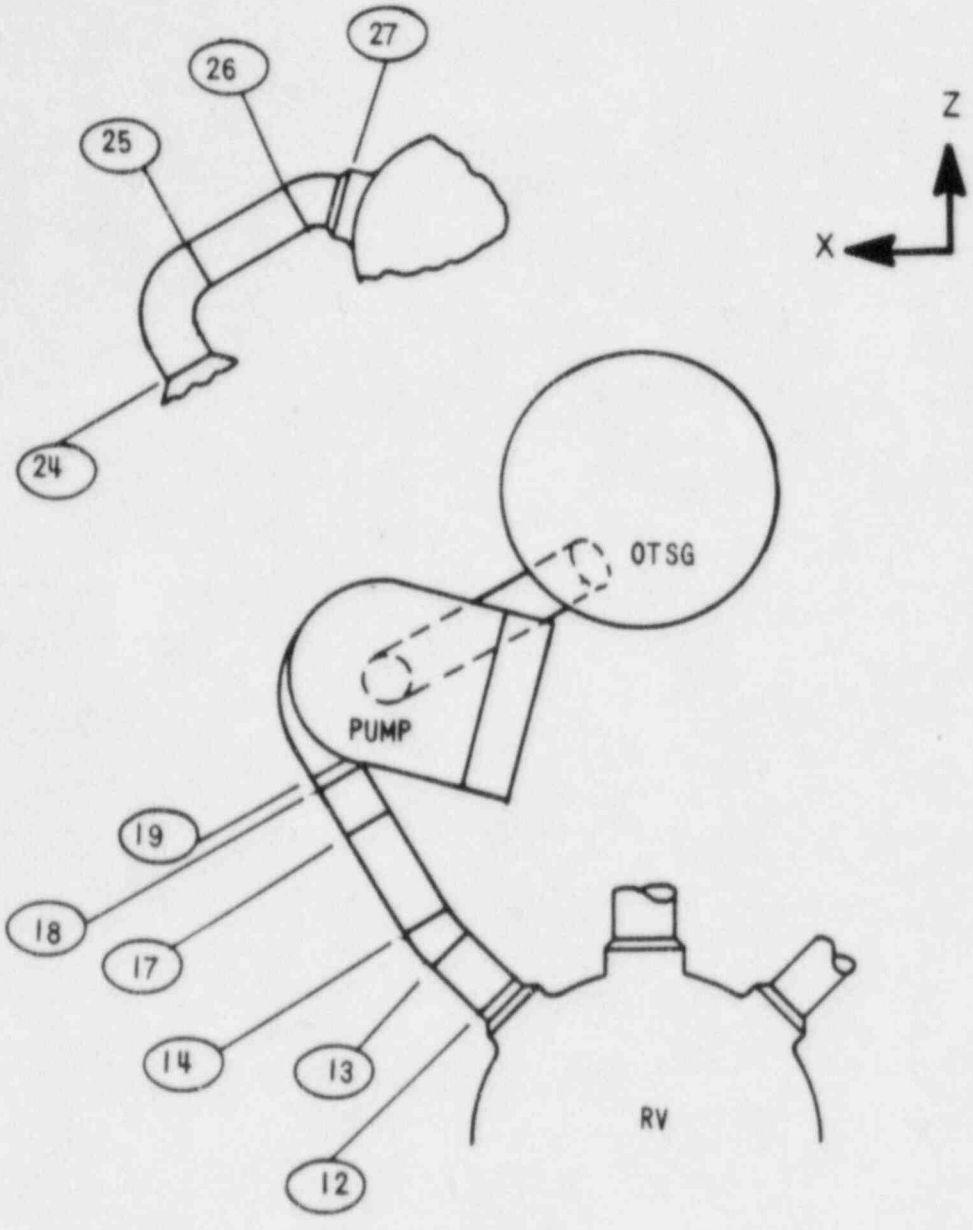

Figure 3-9. 177-FA Plant Lower Loop Hot Leg Weld Locations

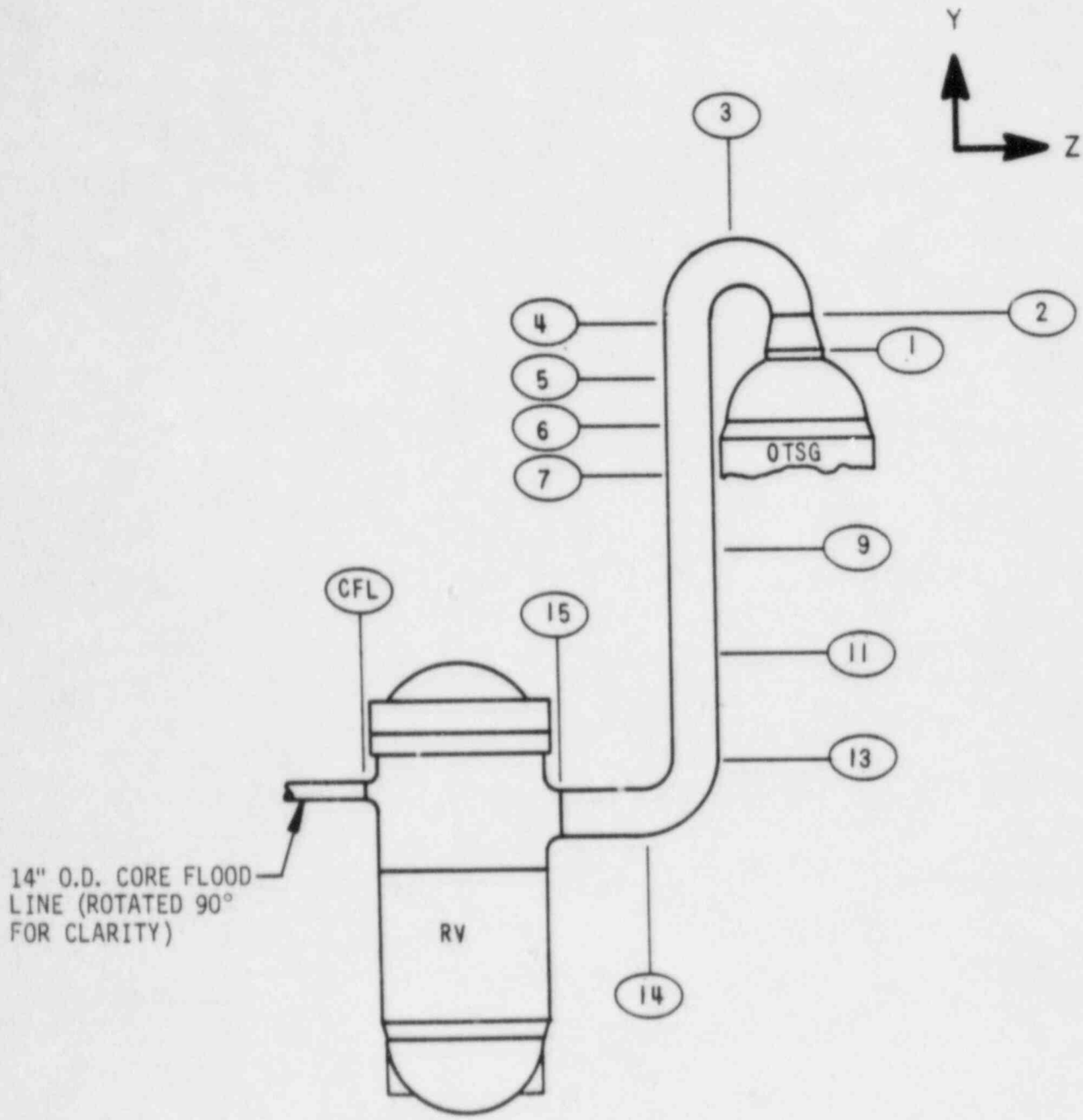

Figure 3-10. 177-FA Plant Lower Loop Cold Leg Weld Locations

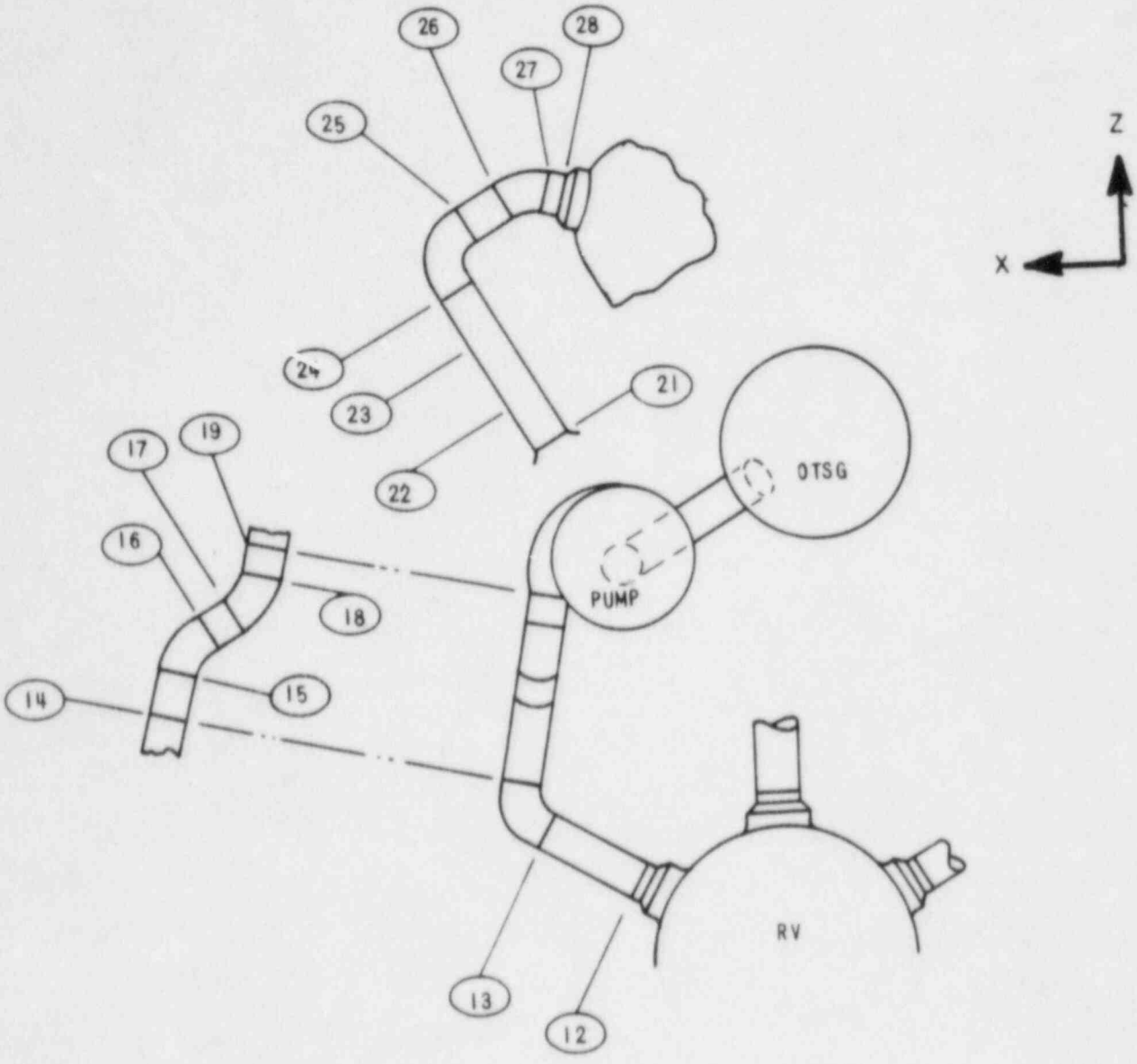

Figure 3-11. Locations, Weld Type and Materials in a Typical B&W Designed NSS

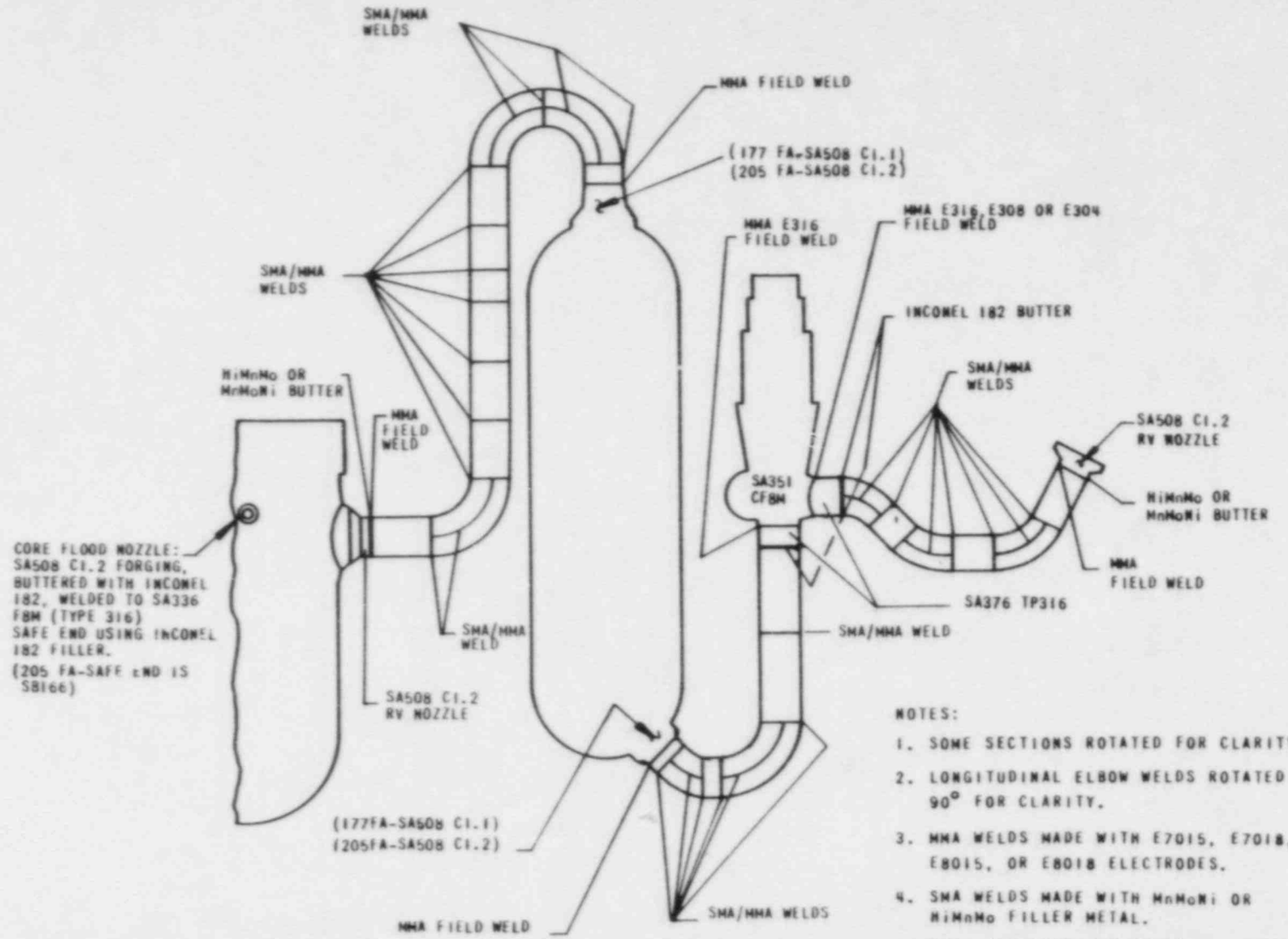

NOTES:

1. SOME SECTIONS ROTATED FOR CLARITY.
2. LONGITUDINAL ELBOW WELDS ROTATED 90° FOR CLARITY.
3. MMA WELDS MADE WITH E7015, E7018, E8015, OR E8018 ELECTRODES.
4. SMA WELDS MADE WITH MnMoNi OR NiMnMo FILLER METAL.
5. STRAIGHT SECTIONS ARE SA106 GR.C.
6. ELBOWS SECTIONS ARE SA516 GR. 70.

Figure 3-12. Illustration of Pipe Geometry

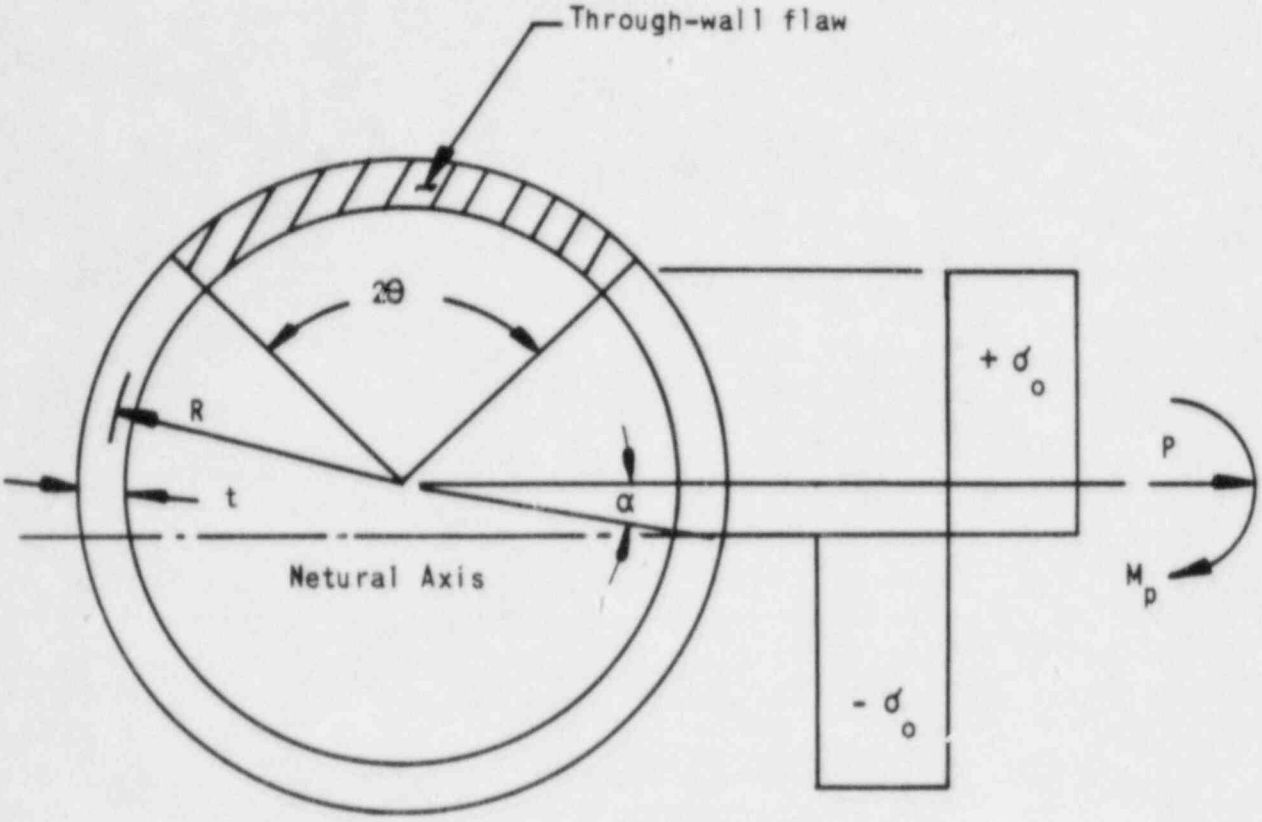

Figure 3-13. Quarter Section of Unrolled Pipe F. E. Model

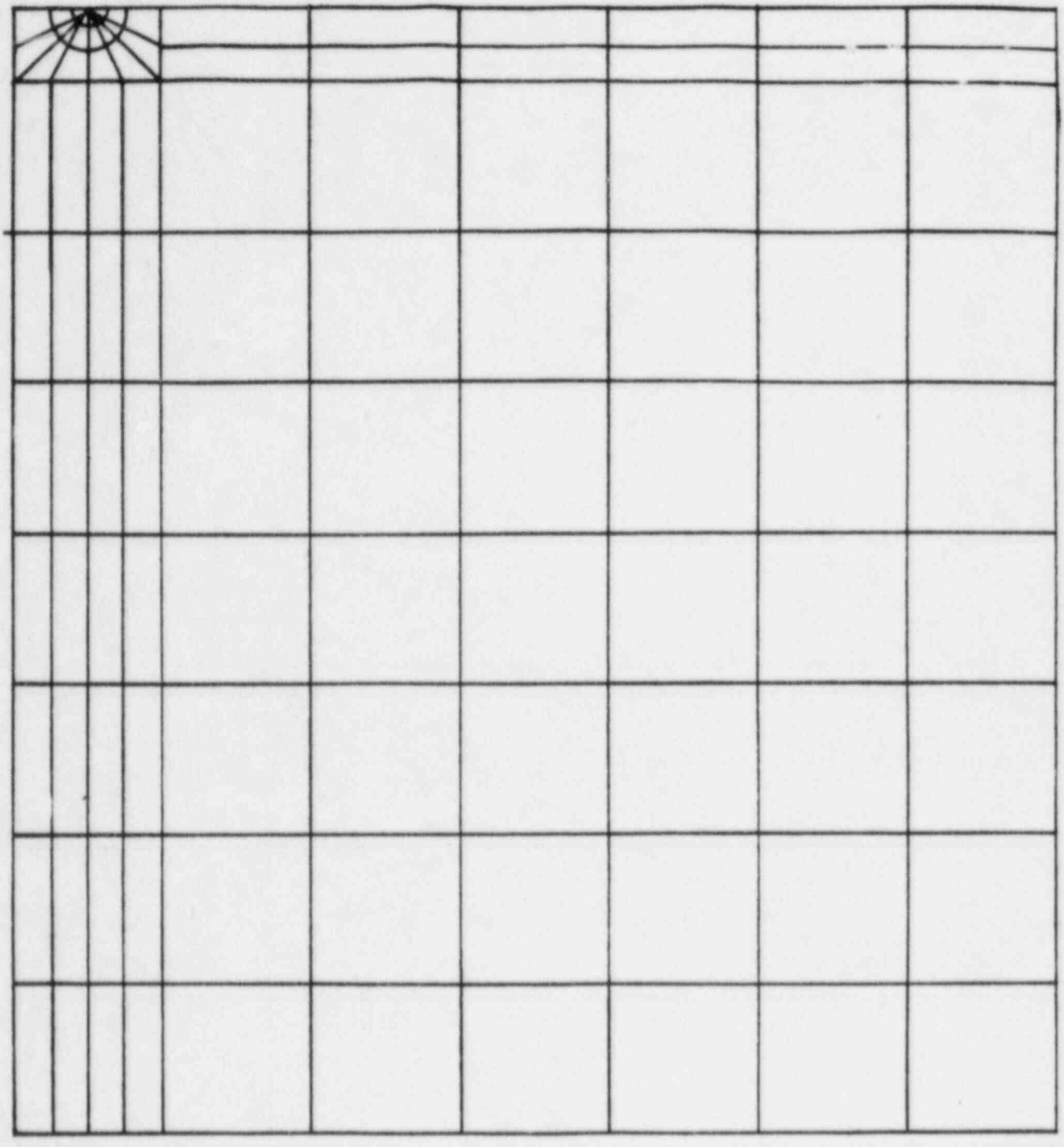

Figure 3-14. Flaw Tip F. E. Model - Element and Node Pattern

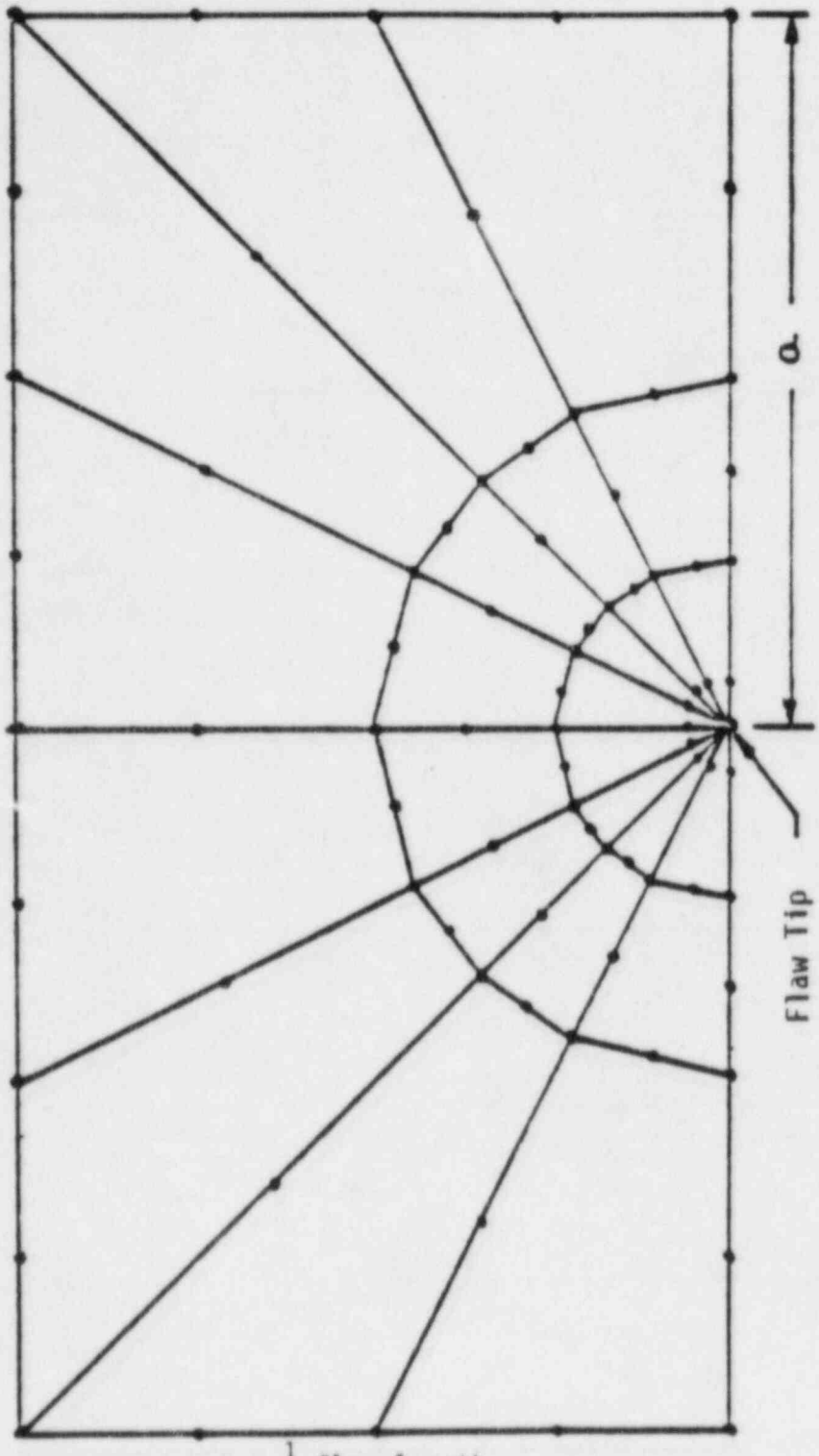

Figure 3-15. Quarter Section of Hot Leg Elbow F. E. Model

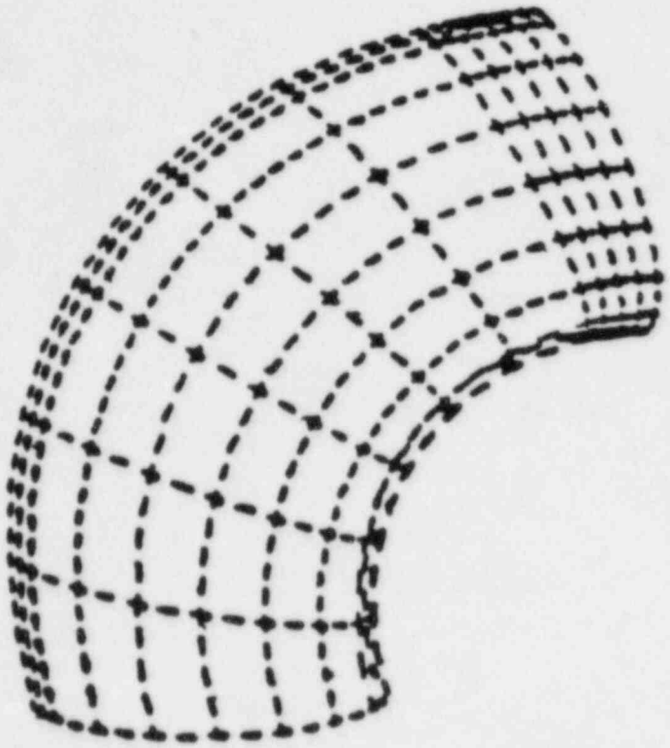

Figure 3-16. Illustration of Stability Assessment Program

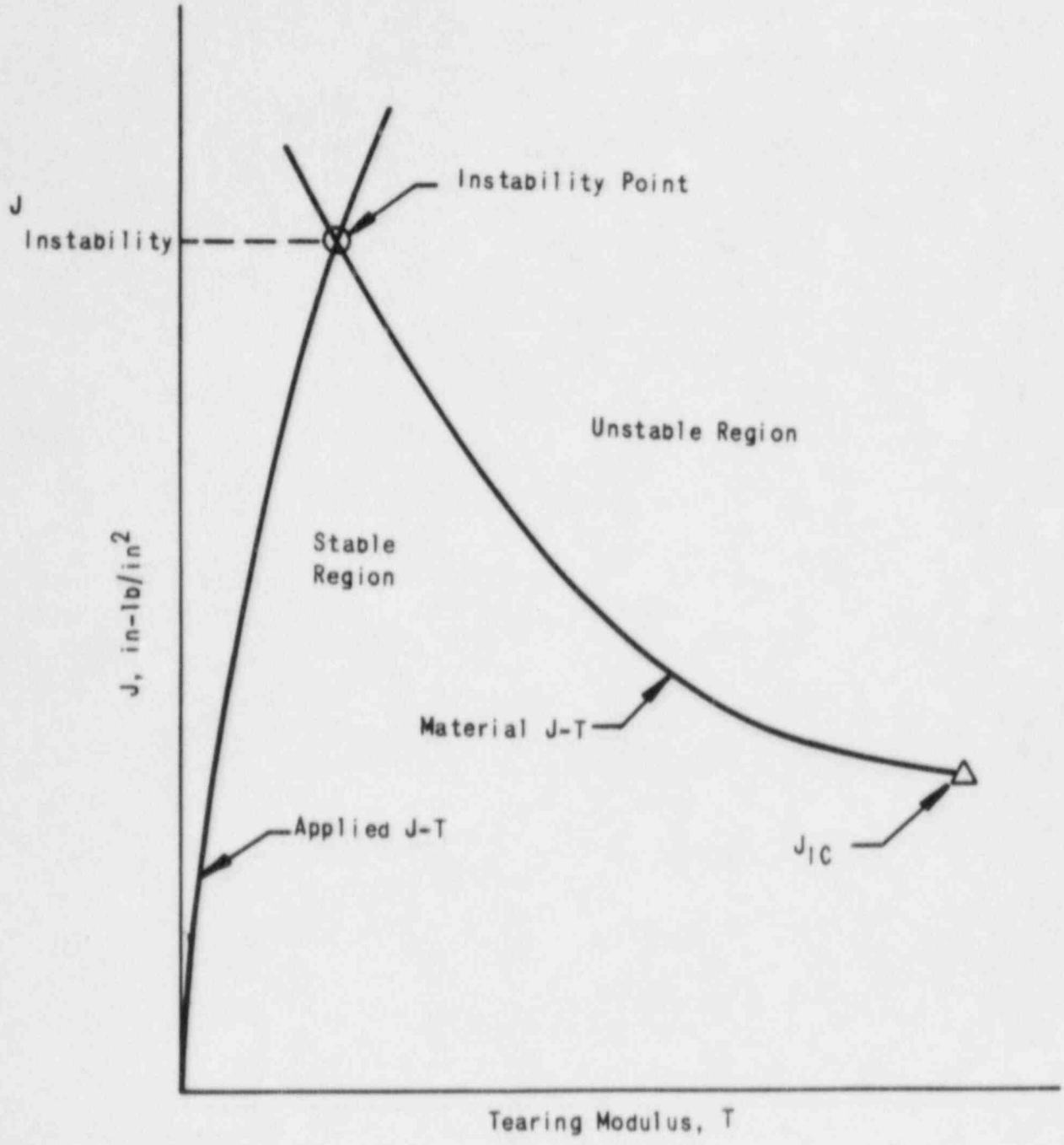

4. LBB EVALUATION RESULTS FOR THE RCS PRIMARY PIPING

This section presents the results of the generic LBB evaluation of the RCS primary piping in the B&WOG plants. The generic LBB results were obtained using bounding loads and base and weld material properties representating all participating B&W utility's plants to ensure that they are enveloped by this evaluation.

4.1. RCS Operating Conditions

For the LBB evaluation, the plant is assumed to be operating under normal full power conditions with a postulated flaw equal to the 10 gpm leakage flaw existing at specific locations in the RCS primary piping. The SSE loads are then added to the normal operating loads to obtain the resultant moment used in the fracture mechanics analysis. Normal system operating conditions used for the LBB analysis were 2150 psi, 600F and RCS flows for the various pipe sizes to bound all 177- and 205-FA plants. However, during the search for the maximum and minimum loads, other hot power conditions in addition to 100% power were considered to ensure obtaining the bounding loads.

Since there are many pipe sizes existing in the 177-FA and 205-FA plants, the 10 gpm leakage flaw was established for each pipe size.

4.2. Leak Rate Versus Flaw Length

Using two load sets, the postulated leakage flaw size was determined for pipe sizes of 28 to 38 inches, inside diameter. This postulated through wall flaw length corresponds to a leak flow rate of 10 gpm in all cases.

An initial scoping flaw size evaluation subjected the pipe to internal pressure only with no bending moments applied producing overly conservative flaw sizes. A second flaw size evaluation was performed to provide an assessment for using more realistic, yet still conservative loading conditions, the actual minimum existing normal operation axial, and bending stresses.

The results of the evaluation with internal pressure only are presented in Figures 4-1 and 4-2. As can be seen, this loading condition yields flaw lengths ranging from four to five times the pipe thickness (5t).

The trend in Figures 4-1 and 4-2 stems from calculating the flaw geometry (flaw area versus flaw length) as modified by the flow calculation. Flaw geometry is a function of the mean radius, R, and the pipe wall thickness, t. Specifically, flaw length and flaw area are related in a complex manner to R/t, Rt, $1/\sqrt{Rt}$. From Table 3-6, it can be determined that R/t does not vary in a monotonically increasing fashion with increasing pipe diameter. Hence, R/t interacts with Rt and $1/\sqrt{Rt}$ in a non-uniform manner when computing flow areas as a function of flaw length.

For the 28 through 38 inch straight pipes, with an average R/t $\sim$6.6, there is little difference in the relationship between flow area and flaw length for various pipe sizes. Thus, the trend in Figure 4-1 is controlled by the pipe wall thickness. That is, for a given flaw length the thinner walled pipe offers less resistance to flow and correspondingly yields a higher flow rate. For elbow pipe sections there is a discernable difference in the relationship between flow area and flaw length with pipe size. For a given flaw length, area is no longer approximately constant with changing pipe size. The trend with pipe size is the same as that shown in Figure 4-2. Therefore, since there is little difference in the wall thickness (or flow resistance) between the 32 and 36 inch elbows the flow calculation is not sufficiently dominant to reverse the 32 and 36 inch curves in Figure 4-2.

The results using a more realistic, although still conservative, set of pipe loading conditions; that is, existing normal operating axial and bending stresses are presented in Figure 4-3 and Table 4-1. The stresses were obtained from the results of the minimum load data at weld locations (equation 3-2) discussed in Section 3.3.1. Figure 4-3 presents the results of this calculation for the 38 inch straight pipe configuration. Table 4-1 shows the flaw lengths corresponding to 10 gpm that was used in the fracture mechanics evaluation described in section 3.3.5. The use of the actual axial and bending stresses provided flaw lengths of approximately three times the pipes' thickness (3t). This calculation is still conservative since minimum existing pipe stresses were used and since the pressure acting on the surface of a crack was not considered.

4.3 Fatigue Flaw Growth Analysis

Results of the fatigue flaw growth analysis discussed in section 3.3.2 are presented in Table 4-2 for the 28 and 38 inch RCS primary piping. These results were based on the input stresses and number of cycles provided in Tables 4-3, 4-4, and 4-5 which were based on the ASME code transients and SSE loads. Table 4-2 shows the minimum surface flaw depth (semi-elliptical shape) which will grow through the pipe wall thus creating a through-wall flaw in the forty years of the design life. For the 28" ID pipe any initial flaw depth (circumferential flaw) less than sixth-tenths of the pipe wall thickness (0.6t) will not extend through-wall during the design life. Likewise, any longitudinal flaw whose depth is less than 0.4t will not become a through-wall flaw during the design life.

It is important to determine if an initial surface flaw will grow in the radial direction to become a through-wall flaw instead of growing in the circumferential (or longitudinal) direction as a part-through flaw. It was shown using the BIGIF code with the variable aspect ratio option, that the preferen-

tial flaw growth is in the through-wall direction of the pipe thereby causing a detectable leak to occur prior to significant circumferential extension.

4.4 RCS Material Properties

Once the B&WOG materials test program defined in section 3.3.4.4 was completed; the results were used in this analysis. This test was conducted under the B&W QA program for material testing. The materials in B&WOG plant RCS piping were divided into two major categories: 1) a group of weld metals and 2) base metals i.e. SA106C and SA516. Tensile, Charpy and compact test specimens are fabricated from materials for a NSS using standard shop fabrication procedure and tested at B&W Alliance Research Center. The test results for the tension, Charpy and compact fracture data are provided in reference 17.

4.4.1 Weld Metal Properties

A total of 18 compact specimens were tested representing three types of weld metals from six different heats. The lowest J-R curve is shown in Figure 4-4 represented by a five parameter equation in the following form:

$$J_R = -6.51393\ (0.085 + \Delta a)^{-2} + 3687.37\ \Delta a + 1197.94$$

where J_R is material $J_{modified}$ in in-lb/in^2 and crack extension Δa in inches. This J-R curve has a J value of 3940 in-lb/in^2 at a maximum crack extension of 0.77 inch. The J-R curves for all other weld metals lie above this curve. The J-R data was obtained at a test temperature of 550F.

Tensile test specimens for the weld metals were machined from the same piece of material used for the compact specimen testing with .25 inch diameter. The tensile specimens were also tested at 550F. Representative results for the tensile properties of interest are:

$$\sigma_y = 76.0 \text{ ksi}$$
$$\sigma_{ult} = 89.5 \text{ ksi}$$

and $\sigma_o = 0.5 (\sigma_y + \sigma_{ult}) = 82.8$ ksi.

While there were some weld metals with lower yield strengths, their toughnesses were higher than those used in the LBB analysis. The above choice can be shown to be the most limiting considering these two competing influences on the J-integral evaluation.

To obtain the Ramberg-Osgood parameters, a true-stress-true strain curve is needed. From the tensile test records, this curve can be constructed as shown in Figure 4-5 for the representative weld metal. The following Ramberg-Osgood equation is fitted to the true stress-true strain curve:

$$\frac{\varepsilon}{\varepsilon_o} = \frac{\sigma}{\sigma_o} + \alpha \left(\frac{\sigma}{\sigma_o}\right)^n$$

where
- σ, ε - true stress, true strain
- σ_o - yield stress
- ε_o - σ_o/E
- E - Young's modulus
- α, n - Ramberg-Osgood material parameters.

The resulting Ramberg-Osgood parameters for the entire strain range of $0. < \varepsilon < 0.15$, where true strain of 0.15 coincides with the maximum load point in the load displacement curve, are:

$\alpha = 0.867$

$n = 14.8.$

If one tries to obtain a fit closer to the lower true strain range, it will result in a higher strain hardening parameter n, as is the case in the following base metal discussed in Section 4.4.2. Since the high range of n (greater than 7) is not defined in the EPRI/GE method, no attempt was made to obtain a better fit closer in the lower strain range.

4.4.2. Base Metal Properties

The test results from four compact test specimens indicate that both base metals, SA106C and SA516, exhibit almost identical J resistance behaviors. Since the straight pipe sections have the highest stress in RCS piping and are fabricated from SA106, the SA106 properties are chosen for the LBB evaluation.

The J-R data can be expressed in the following equation which shows very good correlation as shown in Figure 4-6.

$$J_R = -3.12872\ (0.06 + \Delta a)^{-2} + 5172.63\ \Delta a + 1146.48$$

where J_R is material J modified in in-lb/in^2 and Δa is crack extension in inches. This J-R data have a J value of 4280 in-lb/in^2 at a maximum crack extension of 0.6 inch. All test data was obtained at 550F.

Representative results for the tensile properties of interest for SA106 are:

$$\sigma_y = 39 \text{ ksi}$$

$$\sigma_{ult} = 81 \text{ ksi}$$

and $$\sigma_o = 0.5(\sigma_y + \sigma_{ult}) = 60 \text{ ksi}.$$

For this evaluation the yield strength is used for evaluation of J using the EPRI/GE method. The flow stress σ_o is used for limit load and tearing modulus determination.

The corresponding true stress-true strain curve is shown in Figure 4-7. With a least squares fit to the entire strain range i.e. $0 < \varepsilon < 0.15$ one obtains the following Ramberg-Osgood parameters:

$$\alpha = 1.48$$

$$n = 5.05$$

However, if one chooses to fit the true-stress-true strain curve in the lower strain range, e.g. $0 < \varepsilon < 0.012$, the Ramberg-Osgood parameters become:

$$\alpha = 1.4$$

$$n = 9.0.$$

It can be argued that the latter correlation covers the majority of the RCS piping under analysis and this may explain the difference between the results from the MARC analysis and the EPRI/GE method as shown in Table 4-8.

4.5. Flaw Stability Analysis

4.5.1. Linear Elastic Fracture Mechanics Analysis

As described in section 4.2 four pipe diameters were selected for analyses with the expected maximum forces and moments tabulated in Table 4-6. LEFM analyses were performed for all pipe sizes using the MARC code and Paris-Tada method. The stress intensity factors and the corresponding J values are listed in Table 4-7. The following conversion equation was used to obtain J for LEFM domain;

$$J = K_I^2/E$$

where a plane stress condition was assumed and K_I is stress intensity factor and E is Young's modulus.

Three longitudinal flaws were evaluated to ensure the seam weld joint in all elbows in the "candy cane" sections are considered in the LBB analysis.

For all pipe sizes except the 28 inch straight section, the applied stress intensity factors are less than the K_{IC} determined from J_{IC} data obtained from the materials testing as shown in Table 4-7. Therefore, no flaw initiation occurs and the flaws in these pipes are inherently stable. All stress intensity factors, K_I, are independent of such material parameters like σ_o, α and n. For the 28 inch straight pipe section K_I is greater than K_{IC}, therefore, an elastic-plastic fracture mechanics analysis was performed as discussed in Section 4.5.3.

The maximum applied moment for all pipe sizes is shown in Table 4-6 to be 7253 ft-kip. However, the 38 inch straight section does not have the limiting load because the pipe stress is lower in the 38 inch straight pipe than in the 28 inch straight pipe.

The stress is less in the 38 inch pipe since the piping wall thickness (3.125" vs 2.375) is larger than the 28 inch pipe.

4.5.2 "Candy Cane" Section of Hot Leg Piping

Since the upper hot leg (candy cane section) of the B&W designed NSS contains a double elbow (180° bend) (see Figure 3-2) that is unique to the B&WOG's plants, an evaluation of this section of the RCS piping was performed in detail using finite element analysis. Utilizing symmetry, only a 90° section was modeled by the MARC finite element code, Table 4-7 contains results for these elbow sections of the hot leg piping. The results for the "Candy Cane" sections of the hot leg piping show that the applied stress intensity factors are less than K_{IC} and less than the stress intensity factors of the corresponding straight sections. This is due to the thicker walls of the elbow sections and lower applied loads which reduces the stress level when compared with the corresponding straight sections of piping.

4.5.3 Tearing Instability Analysis

To perform a tearing instability analysis, a J versus tearing modulus (J-T) diagram must be generated showing both the material J-T and applied J-T curves for determination of the J at the instability point.

Since applied K_I values indicate that the 28 inch cold leg pipe flaw is in the EPFM range, this was analyzed by EPFM methods, the applied J values were calculated by the EPFM option in the MARC code and the EPRI/GE method. Since a finite element analysis is not well suited for tearing modulus calculation and requires considerable efforts to compute a J value, the EPRI/GE method is used to generate the applied J-T diagrams for tearing instability analysis. In applying the EPRI/GE method, the applied force including the end cap pressure effect and moment shown in Table 4-6 are combined into an equivalent moment by the following equation suggested by ref. 18:

$$M_{eq} = M + 0.5\ R\ F_t/F_b\ P$$

where M - applied moment

R - radius of pipe

F_b - geometry factor for K_I in bending

F_t - geometry factor for K_I in tension

P - axial force.

On the other hand, the finite element analysis was performed with the given load set without converting the axial force into an equivalent moment. The J-T diagrams constructed for weld and base metals are shown in Figures 4-8 and 4-9. The material J-T curves are based on the J_R equations given in section 4.4 for the weld and base metals. It is shown that the $J_{instability}$ for both weld and base metals are greater than a J value of approximately 4000 in-lb/in^2. At this point an alternate limit on J, called $J_{upper\ limit}$ (J_{UL}), is introduced based on a maximum crack extension from an actual compact test specimen data. From Figures 4-4 and 4-6 and in section 4.4, J_{UL} of 3940 and 4280 in-lb/in^2 are established for weld and base metals at the maximum crack extensions of 0.77 and 0.6 inches, respectively. This maximum crack size is not necessarily the limit as noted in the Degraded Piping Program (ref. 19) which showed more than one and a half inch of stable tearing from 3T compact specimen testing.

Whenever the applied J is limited by this J_{UL}, tearing stability is assured because $J_{instability}$ is greater than J_{UL}.

The resulting J versus moment diagrams for the 28 inch straight cold leg piping using the EPRI/GE method are presented in Figures 4-10 and 4-11. Using the equivalent moment loading of 50.26×10^6 in-lbs., both weld and base metal cases show applied J values of 601 and 888 in-lb/in^2 respectively. The applied J for the base metal case of 888 is higher than the MARC EPFM J value of 677 by (31%), however, both cases show adequate margin against J_{UL}.

In the EPRI/GE method the J plastic term is sensitive to the Ramberg-Osgood parameters (α, and n) and yield stress for high moments. For the parameter n near 5, this approach results in a conservative J calculation when compared with the finite element analysis. With weld metal properties and n greater than 9, the J values remain in the elastic range. This leads us to believe that the J-moment relationship for the base metal case is conservative (Figure 4-11).

The MARC EPFM analysis for the 28 inch cold leg using the moment and the axial tensile force loads listed in Table 4-6 yields an applied J of 677 in-lb/in^2 for the base metal. In addition, an analysis with the loads multiplied by the square root of 2, a safety factor suggested by NUREG-1061, Vol. 3, results in an applied J of 2096 in-lb/in^2 which is less than the J_{UL} of base metal shown in Table 4-8. The corresponding loads versus J curve for the 28 inch pipe with the base metal properties is presented in Figure 4-12.

A reason for the discrepancy between the finite element and the EPRI/GE method may lie in the Ramberg-Osgood representation of the stress-strain relationship of the material which is required by the EPRI/GE method. Fitting a specific true stress-true strain data with the Ramberg-Osgood equation becomes an issue because of its non-unique nature. As described in section 4.4.2, a different set of Ramberg-Osgood parameters, which fits the true stress-true strain curve better near the yield stress, may be a better representation of the material under consideration. This latter set of Ramberg-Osgood parameters yields a J value of 675 in-lb/in^2 which is very close to the MARC EPFM result.

In Table 4-9 all four straight pipe sections are compared with the K_I/J calculated by the EPRI/GE and other methods. When the base metal properties are used (when n is low), the EPRI/GE method results in a very large J plastic term which is expected to be negligible when K_I is less K_{IC}. This leads us to believe

that the EPRI/GE method becomes very conservative when the hardening parameter n is low. A non-agreement between the EPRI/GE method and test data for compact specimens was also mentioned (in ref. 19). Therefore, the final safety margins in this LBB evaluation are assessed using the results from the finite element analysis.

4.6. Safety Margins in RCS Primary Piping

4.6.1. Margin on Loads

To assess the safety margins on load, it is necessary to determine the J at the instability point. However, as discussed in section 4.5.3 only the upper limit value of J was obtained for the point of the largest crack length. Through LEFM analyses only the 28 inch straight pipe section was identified as the case where the applied K_I exceeds the K_{IC} as shown in Table 4-7. For the remaining seven pipe sizes, it was shown that the applied stress intensity factors were lower than the K_{IC} and hence the safety margins are greater than the safety margin of the 28 inch straight pipe section.

The safety factor on loads is defined as the ratio between the load which correspond to J equal to J_{inst}, and the applied loads. This safety factor on load can be evaluated from the J vs. loads diagram shown in Figure 4-12. This J vs. loads curve is constructed from the MARC finite element analysis for 28 inch straight pipe using the base metal true stress-true strain curve and actual moment, axial force and internal pressure as input. The points on the curve are from the incremental applied loads ranging from a fraction of the applied loads to 1.414 times the applied loads, as was recommended by NUREG-1061, Vol. 3. The applied J value at the last point is 2096 in-lb/in^2 which is much less than the J_{UL} of 4280 in-lb/in^2. This indicates that this pipe section is stable even under the increased load level of 1.414 times the actual load set. Thus, a safety factor on loads greater than 1.414 exists

with respect to J_{UL}. Even the conservative J-moment relationship from the EPRI/GE method yields adequate margin of safety as shown below:

1) For base metal

$$S.F. = \frac{\text{Moment (where } J=J_{UL})}{\text{Applied Moment}} = \frac{71.06 \times 10^6}{50.264 \times 10^6} = 1.414$$

2) For weld metal

$$S.F. = \frac{\text{Moment (where } J=J_{UL})}{\text{Applied Moment}} = \frac{112.2 \times 10^6}{50.264 \times 10^6} = 2.23$$

where the effects of crack extension were included in these factors. Since the 28 inch pipe case was the most limiting, the remaining pipe sizes will have safety factors greater than 1.414.

4.6.2. Margin on Flaw Sizes

To assess the safety margins between the critical flaw size and the postulated initial flaw size based on 10 gpm leak rate, the flaw size needs to be incrementally extended until the applied J reaches the value of the J upper limit. This final flaw size is the critical flaw size. This assessment should be performed for the 28 inch cold leg piping.

Since it is costly to make multiple finite element analyses with varying flaw size, an inference is made using the EPRI/GE method with the base metal properties. A flaw size of 20.2 inches yields an applied J value of 4174 in-lb/in^2 which is close to J_{UL}, therefore, the critical flaw size for the 28 inch pipe is 20.2 inches as shown in Table 4-10. Since the assumed initial flaw size was 9.2 inches, the resulting safety factor on flaw size is 2.2. Similarly, it can be shown that the weld metal case yields a safety factor of 4.0. Both factors are greater than the recommended factor of 2 in NUREG-1061, Vol. 3. Since this 28 inch cold leg has the highest stress of all piping sections, the remaining piping sections will have safety factors greater than 2.0.

4.7. Limit Load Analysis

As discussed in section 3.3.6 the limit moments for straight sections of pipes were calculated based on the flaw sizes. The resulting safety factor, the limit moment divided by the applied moment, is tabulated for each pipe size in Tables 4-11 and 4-12 for the weld and base metals. All cases show a factor of 2.7 or greater by this load criteria. The equations used for limit load calculations are valid only for straight sections, however, the results from the straight sections bound the elbows because of the lower stresses in the elbows due to the thicker walls.

A similar evaluation was made on flaw size. The flaw size was increased until the applied moment became equal to the limit moment of the flawed pipe section while the constant axial force remained active throughout. These results are also tabulated in Tables 4-11 and 4-12. All cases show safety factors on flaw size of 3.5 or greater by this criteria.

These results show ample margins of safety in terms of limit loads for the B&W Owners Group RCS Piping with postulated 10 gpm through-wall flaws.

4.8. Conservatisms in LBB RCS Piping Evaluation

Since several disciplines are involved in the LBB evaluation, each with its own inherent conservatisms, a list of items that injects conservatisms into the final LBB results are listed below:

- In obtaining the applied loads for input to the fracture mechanics analysis, the maximum forces and moments and their directional components are summed by the square root of the sum of the squares (SRSS) method which results in conservative loads.
- Worst case sums of various loads were used, since absolute values of the maximum thermal plus deadweight loads are added to the SSE loads.

- The assumption that a through-wall flaw exists in the piping for determination of the applied J-integral.
- Flaw size was determined using a 10 gpm leak rate rather than the 1 gpm sensitivity of the leakage rate detection system, as required by NRC Reg. Guide 1.45.
- Use of a lower bound material J-R curve in each category.
- Axial loading stresses were not included in determination of leakage rate flaw size, however, actual stresses due to end cap pressure were included.
- Maximum steady state SSE values were used in the evaluation and are larger than dynamic (time response) SSE values.

Table 4-1. Leakage Flaw Sizes for Various RCS Pipes

Pipe ID, in.	Minimum moment, ft-kips	Internal pressure, psi	Flaw length (pressure & min. loads), in.
38S	2407	2150	9.0
	991	2150	10.4
38E	916	2150	12.3
	1890	2150	12.0
36S	2284	2150	8.0
	1010	2150	9.8
36E	1010	2150	10.8
32S	1159	2150	9.2
32E	1122	2150	10.6
28S	560	2150	9.2
	1095	2150	7.9
	1246	2150	7.7
28E	1246	2150	9.0
	871	2150	9.6
	1278	2150	9.0

S = straight section of pipe.

E = elbow section of pipe.

Table 4-2. Flaw Sizes Required to Grow Through-Wall in 40 Years

Pipe ID	Thickness	Circumferential flaw	Longitudinal flaw
28"	2.375"	1.33" (.6t)	0.88" (.4t)
38"	3.125"	1.15" (.4t)	1.02" (.3t)

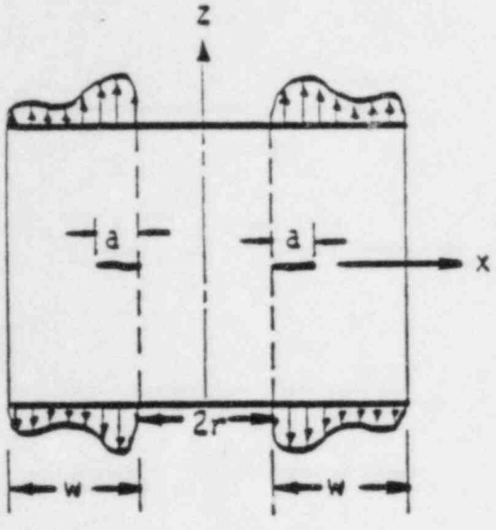

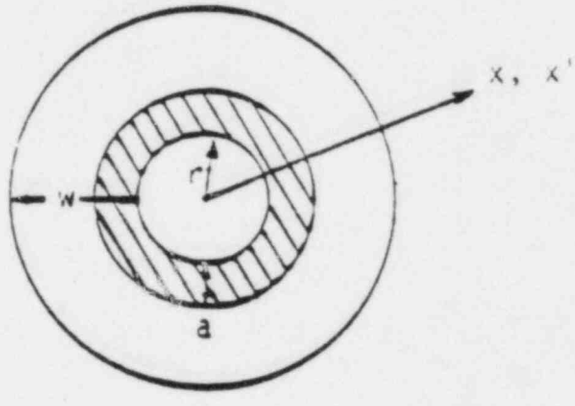

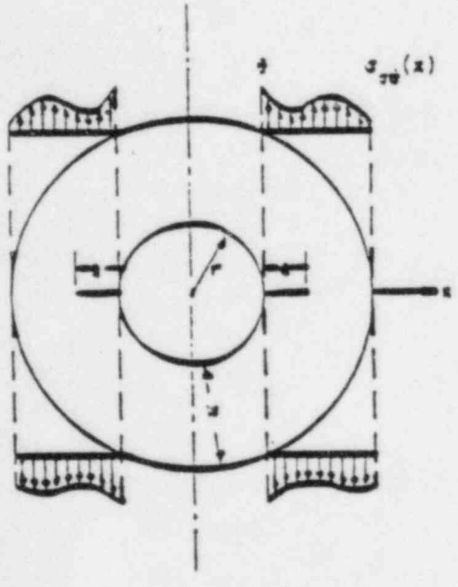

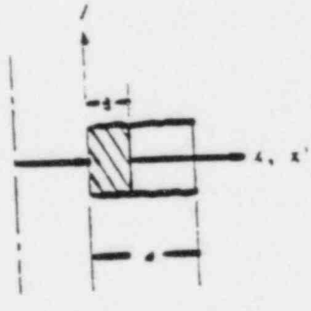

Table 4-3. Design Transients Input to Fatigue Flaw Growth Analysis

Loading condition & location	Number of cycles		Stress, σ_L (psi)	Stress, σ_C (psi)	Stress, σ_L (psi)	Stress, σ_C (psi)
Heatup & cooldown DW&THM Expansion & pressure @ inner surface	240	Max.	9103.	15663.	18173.	15210.
		Min.	0.	0.	0.	0.
DW&THM & pressure @ outer surface	240	Max.	9399.	13413.	19968.	12960.
		Min.	0.	0.	0.	0.
SSE inner surface	22	Max.	16889.	0.	8183.	0.
		Min.	405.*	0.	219.*	0.
SSE outer surface	22	Max.	19433.	0.	9364.	0.
		Min.	358.*	0.	82.*	0.

*Minimum value input to BIGIF for transient is conservatively taken to be zero.

Table 4-4. Plant Design Transient for 40-Year Life - 28-Inch Cold Leg Straight Section

Group	Number of cycles	σ inside, psi	σ outside, psi
I	240	1052	500
II	40	1759	1652
III	428	3876	1383
IV	57770	1052	500

Table 4-5. Plant Design Transient for 40-Year Life - 38-Inch Hot Leg Straight Section

Group	Number of cycles	σ inside, psi	σ outside, psi
I	240	2275	1072
II	572	13566	1072
III	430	9441	1106
IV	58000	2414	1016

Table 4-6. Maximum Applied Forces, Moments and Flaw Sizes Used in Fracture Mechanics Analysis

Pipe size ID, in.	Flaw size, in.	Flaw angle degrees	Axial force* kips	Moment, ft-kips
28 Straight	9.2	17.2	250.3	3098.0
Elbow	9.0	16.5	539.3	2822.8
32 Straight	9.2	15.0	475.2	2260.0
Elbow	10.8	17.0	315.2	2080.0
36 Straight	8.0	11.6	123.3	3952.3
Elbow	10.8	15.5	335.8	2376.5
38 Straight	9.0	12.4	246.6	7253.2
Elbow	12.3	16.7	691.7	3882.6

*Internal pressure generates an additional axial force which is included in the analysis.

Table 4.7 LEFM Analysis Results

Pipe size ID	Circumferential Flaw				Longitudinal Flaw	
	K_I/J_I[1] MARC	K_I by Paris-Tada	J^E by EPRI/GE[2]	K_{IC}/K_I	K_I/J_I MARC	K_{IC}/K_I[3]
38" Straight	104/410	113	492	1.05	-	-
38" Elbow	70/184	-	-	1.21	91/308	1.21
36" Straight	73/203	78	245	1.51	-	-
36" Elbow	56/117	-	-	1.96	88/287	1.25
32" Straight	-	80/238	235	1.38	-	-
32" Elbow	-	-	-	-	-	-
28" Straight	118/529	131	601	0.93	-	-
28" Elbow	87/286	-	-	1.26	80/244	1.37

[1] K_I, ksi $\sqrt{in}$ and J_I, in-lb/in^2

[2] Only the elastic J term using equivalent moment loading.

[3] K_{IC} = 110 ksi $\sqrt{in}$ based on J_{IC} = 451 in-lb/in^2 which is the lower of base and weld metals.

Table 4.8 Results of EPFM Analyses on 28 Inch Straight Pipe

Type of Analysis	J for Load set #1* (in-lb/in^2)	J for Load set #2** (in-lb/in^2)	Stress-Strain Input
MARC Finite Element Analysis	677	2096	Base Metal True Stress Strain
EPRI/GE Weld Metal Prop.	601	1202	α = 0.897 n = 14.8 σ_y = 76 ksi
EPRI/GE Base Metal Prop. A	888	3540	α = 1.48 n = 5.05 σ_y = 39 ksi
EPRI/GE Base Metal Prop. B	675	3576	α = 1.4 n = 9.0 σ_y = 39 ksi

* Load set #1
For MARC: Moment = 37171 (in-kip)
Force = 1685.7 (kip)
For EPRI/GE: Moment = 50264 (in-kip)
Force = 0

**Load set #2 = $\sqrt{2}$ x (load set #1)

Table 4-9. EPRI/GE Method Versus Other Methods (Circumferential Flaws)

Pipe Size ID	K_I/J_I MARC[1]	K_I by Paris-Tada	EPRI/GE Method: Weld Metal J^E	Weld Metal J^P	Weld Metal Prop. J^{total}	Base Metal J^E	Base Metal J^P	Base Metal Prop. J^{total}
38" Straight	104/410	113	492	0	492	490	122	612
36" Straight	73/203	78	245	0	245	245	18	263
32" Straight	--	80/238	235	0	235	235	15	250
28" Straight	118/529 677[2]	131	601	0	601	601	287	888

[1]MARC LEFM Calculation. K_I in ksi $\sqrt{in}$ and J_I in in-lb/in^2.

[2]MARC EPFM Calculation

Table 4-10. Critical Flaw Size Determination
28 Inch Pipe, Base Metal

1/2 Flaw size (in.)	J^E	J^P	J_{total}	J/J_{UL}
4.6	601	287	888	0.208
8.0	1045	1205	2251	0.526
9.8	1280	2521	3801	0.888
9.9	1293	2627	3921	0.916
10.0	1306	2738	4045	0.945
10.1	1319	2854	4174	0.975
10.2	1332	2975	4308	1.006

Applied M = 50.264 (10^6 in-lb)

J_{UL} = 4280 (in-lb/in^2)

28 Inch Pipe, Weld Metal

1/2 Flaw size (in.)	J^E	J^P	J_{total}	J/J_{UL}
4.6	601	0	601	0.153
10.0	1306	0	1306	0.332
18.5	2417	1434	3851	0.977
18.6	2430	1642	4072	1.033
18.7	2443	1881	4324	1.097

Applied M = 50.264 (10^6 in-lb)

J_{UL} = 3940 (in-lb/in^2)

Table 4-11. Limit Load Analysis for Weld Metal

Safety Factors - Limit Moment/Applied Moment

Pipe ID (in)	1/2 Flaw size (in)	Forcex* (kip)	Applied M (in-kip)	Limit M (in-kip)	Safety Factor
28	4.6	250.3	37171	141409	3.8
32	4.6	475.2	27120	221080	8.2
36	4.0	123.3	47428	319971	6.7
38	4.5	246.6	87038	384975	4.4

Safety Factors - Max Flaw Size/10 gpm Flaw Size
(Limit Moment w/max Flaw = Applied Moment)

Pipe ID (in)	1/2 Flaw Size (in)	Forcex (kip)	Appl. M (in-kip)	1/2 Flaw Angle	Crit. Flaw Angle	Safety Factor
28	4.6	250.3	37171	17.2	73.5	4.3
32	4.6	475.2	27120	15.0	86.3	5.7
36	4.0	123.3	47428	11.6	84.9	7.3
38	4.5	246.6	87038	12.4	76.6	6.2

Flow Stress = 82.8 (ksi)

Internal Press = 2.25 (ksi)

*Forcex - applied axial force excluding internal pressure effect

Table 4-12. Limit Load Analysis for Base Metal

Safety Factors - Limit Moment/Applied Moment

Pipe ID (in)	1/2 Flaw size (in)	Forcex (kip)	Applied M (in-kip)	Limit M (in-kip)	Safety Factor
28	4.6	250.3	37171	99690	2.7
32	4.6	475.2	27120	155949	5.8
36	4.0	123.3	47428	227528	4.8
38	4.5	246.6	87038	273534	3.1

Safety Factors - Max Flaw Size/10 gpm Flaw Size
(Limit Moment w/max Flaw = Applied Moment)

Pipe ID (in)	1/2 Flaw Size (in)	Forcex (kip)	Appl. M (in-kip)	1/2 Flaw Angle	Crit. Flaw Angle	Safety Factor
28	4.6	250.3	37171	17.2	60.4	3.5
32	4.6	475.2	27120	15.0	75.4	5.0
36	4.0	123.3	47428	11.6	73.7	6.3
38	4.5	246.6	87038	12.4	63.9	5.2

Flow Stress = 60 (ksi)

Internal Press = 2.25 (ksi)

Figure 4-1. Leak Flow Rate Versus Crack Length for Straight Pipes Subject to Internal Pressure Only

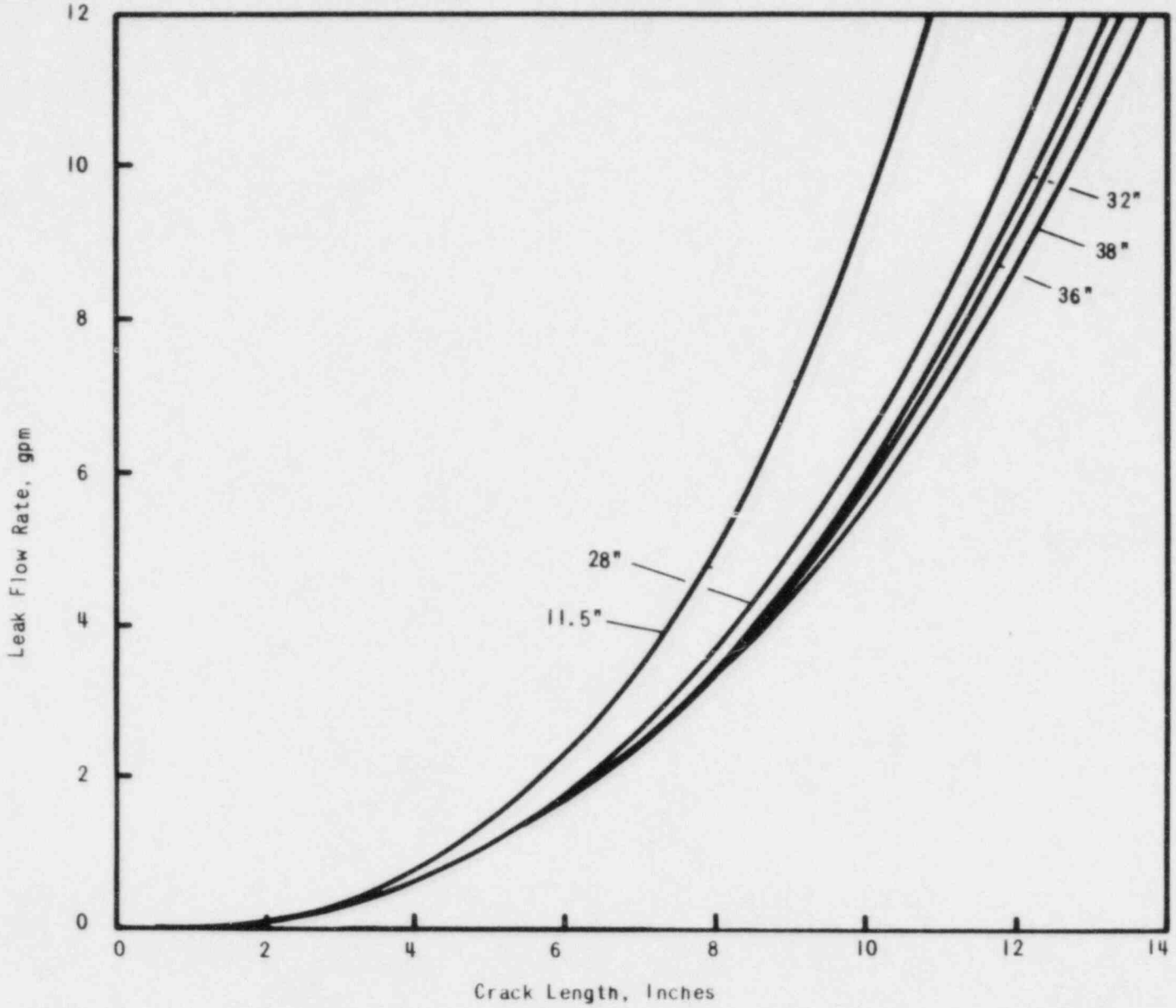

Figure 4-2. Leak Flow Rate Versus Crack Length for Elbows Subject to Internal Pressure Only

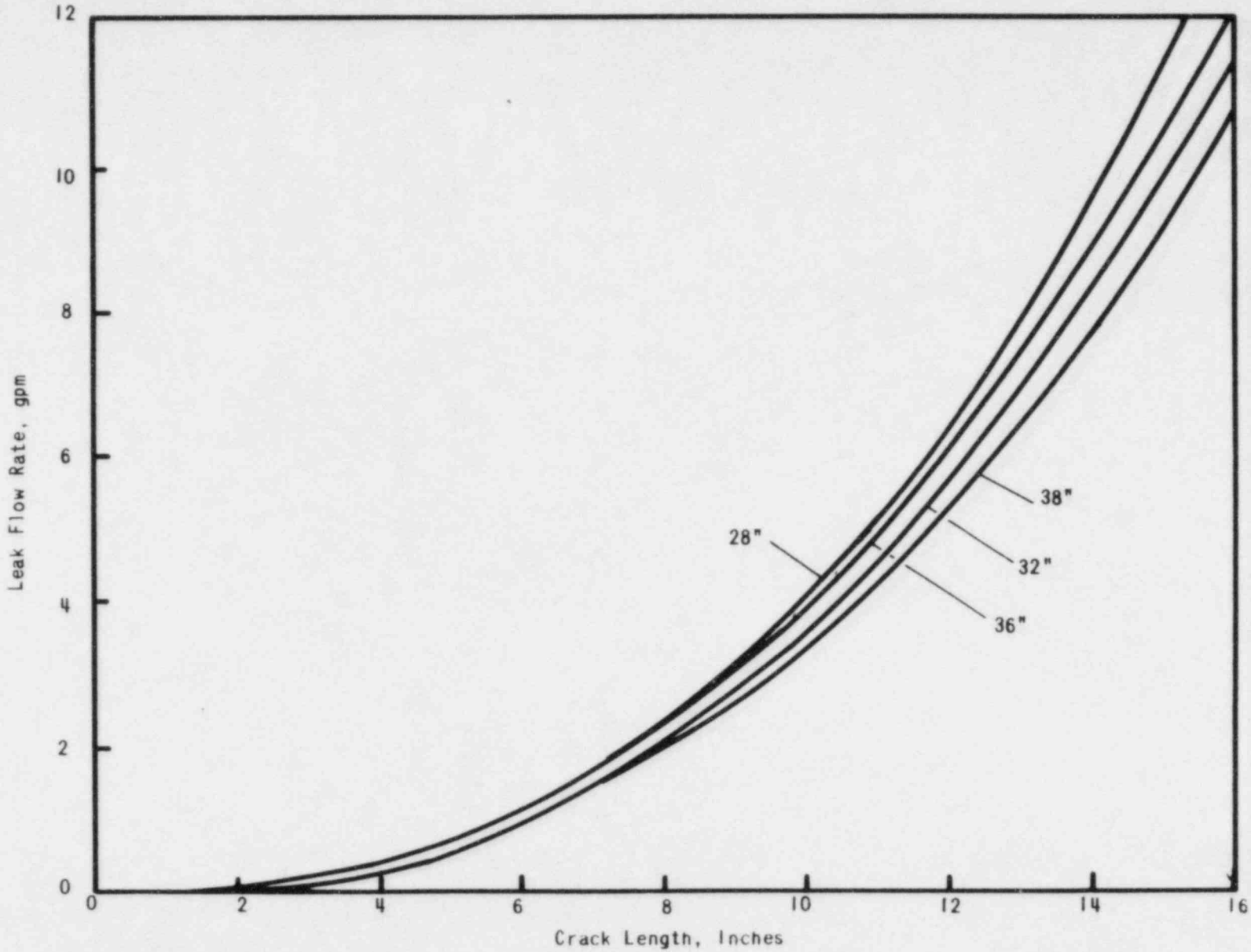

Figure 4-3. Leak Rate Vs Flaw Length for a 38" Straight Pipe Subjected to an Axial Stress of 6.41 ksi and Various Bending Stresses

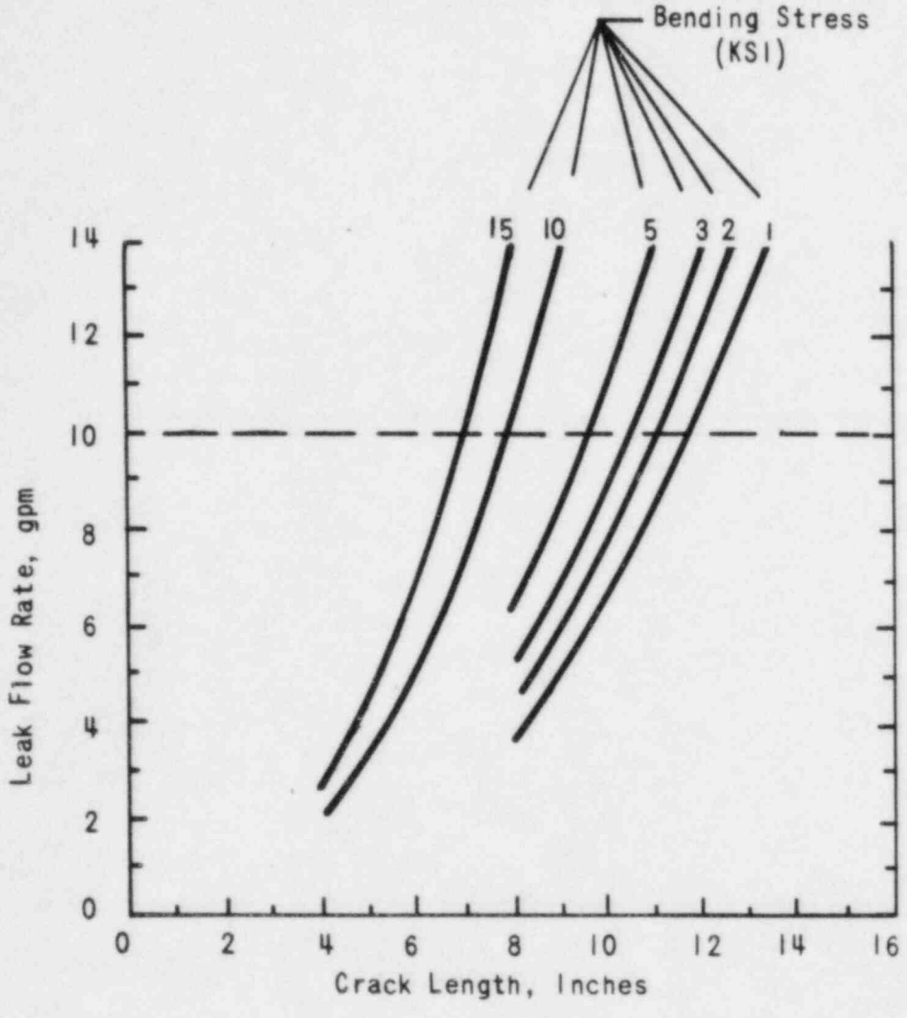

Figure 4-4. J-R Curve for Weld Metal

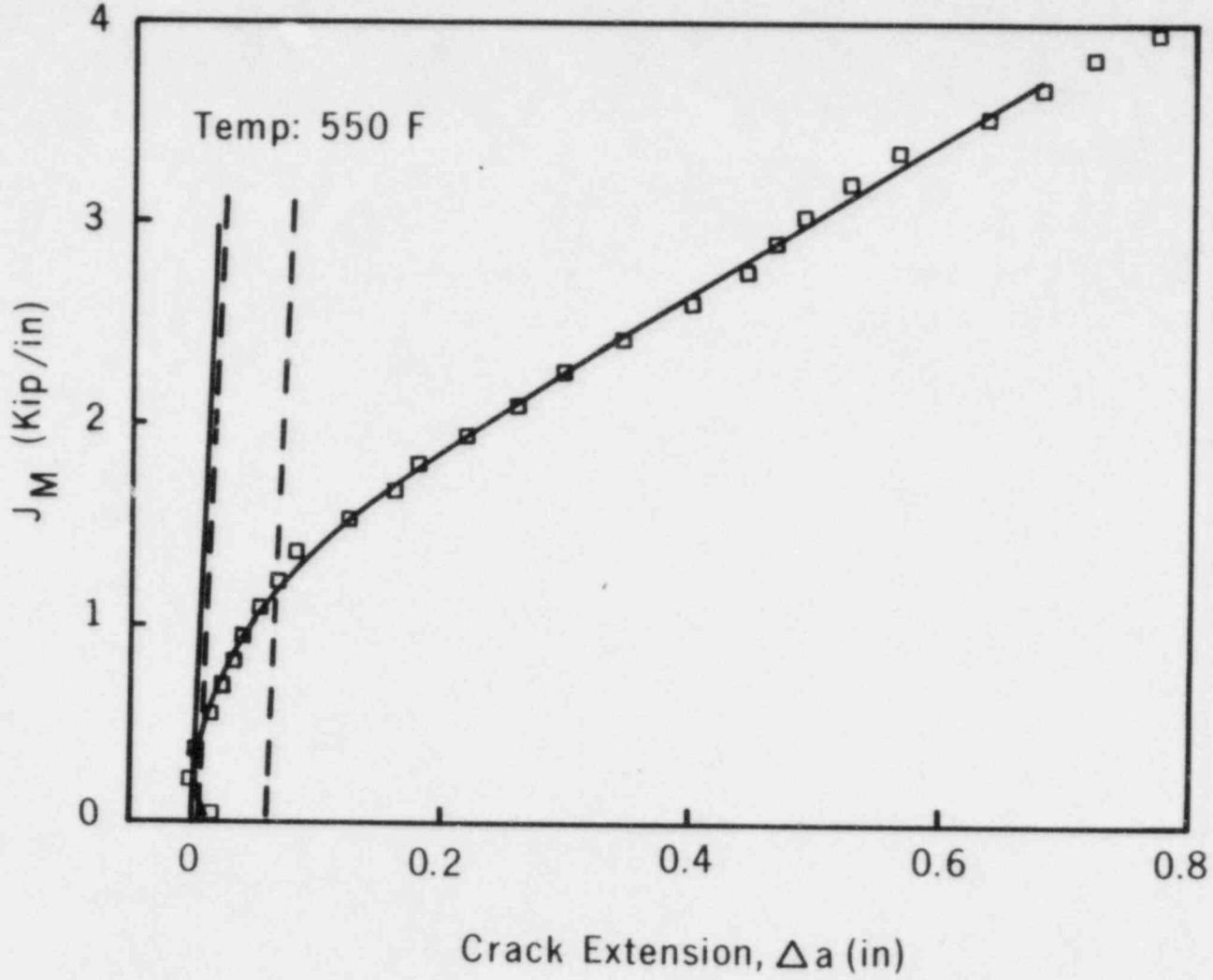

Figure 4-5. True Stress-True Strain Curve for Weld Metal

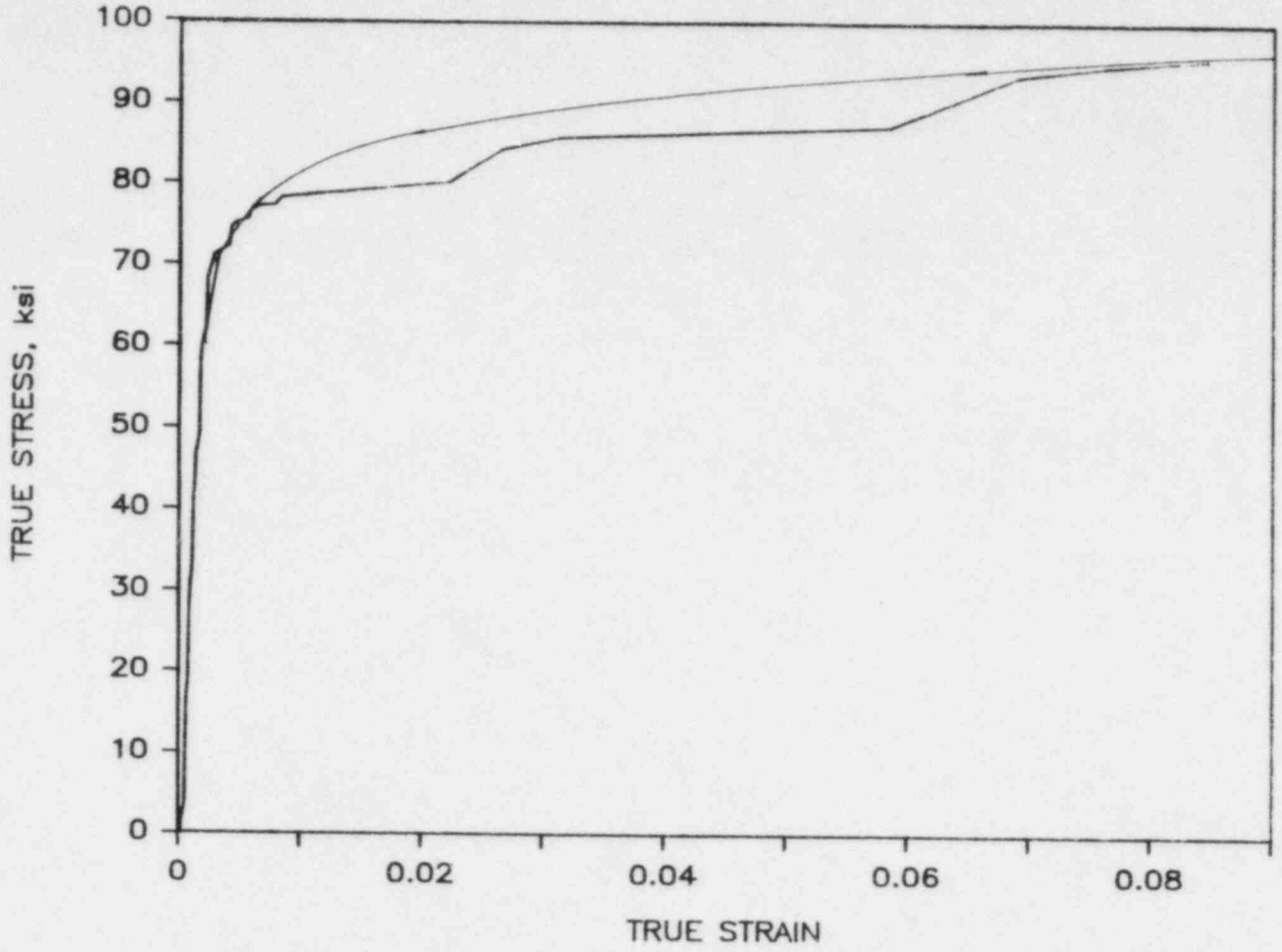

Figure 4-6. J-R Curve for Base Metal

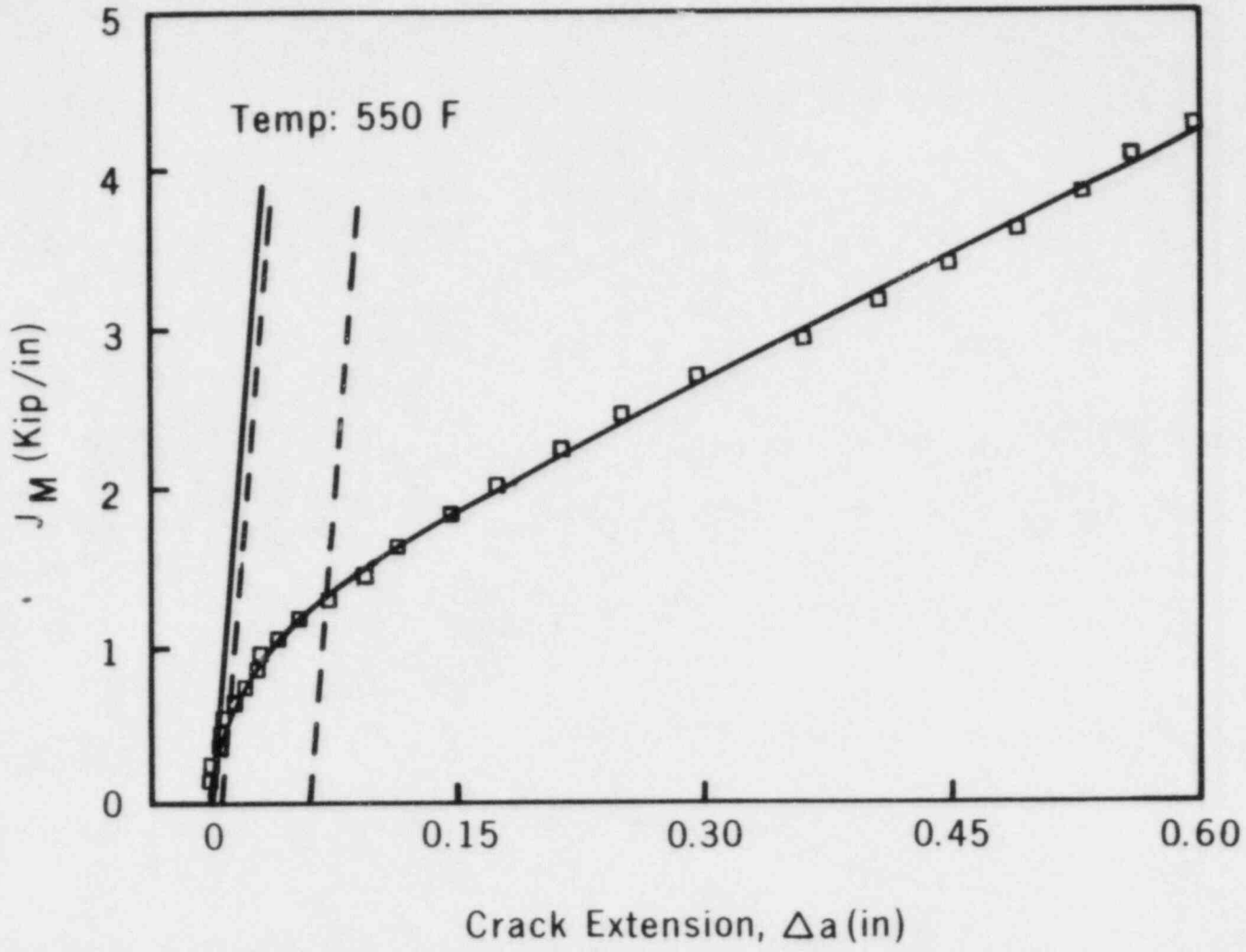

Figure 4-7. True Stress-True Strain Curve for Base Metal

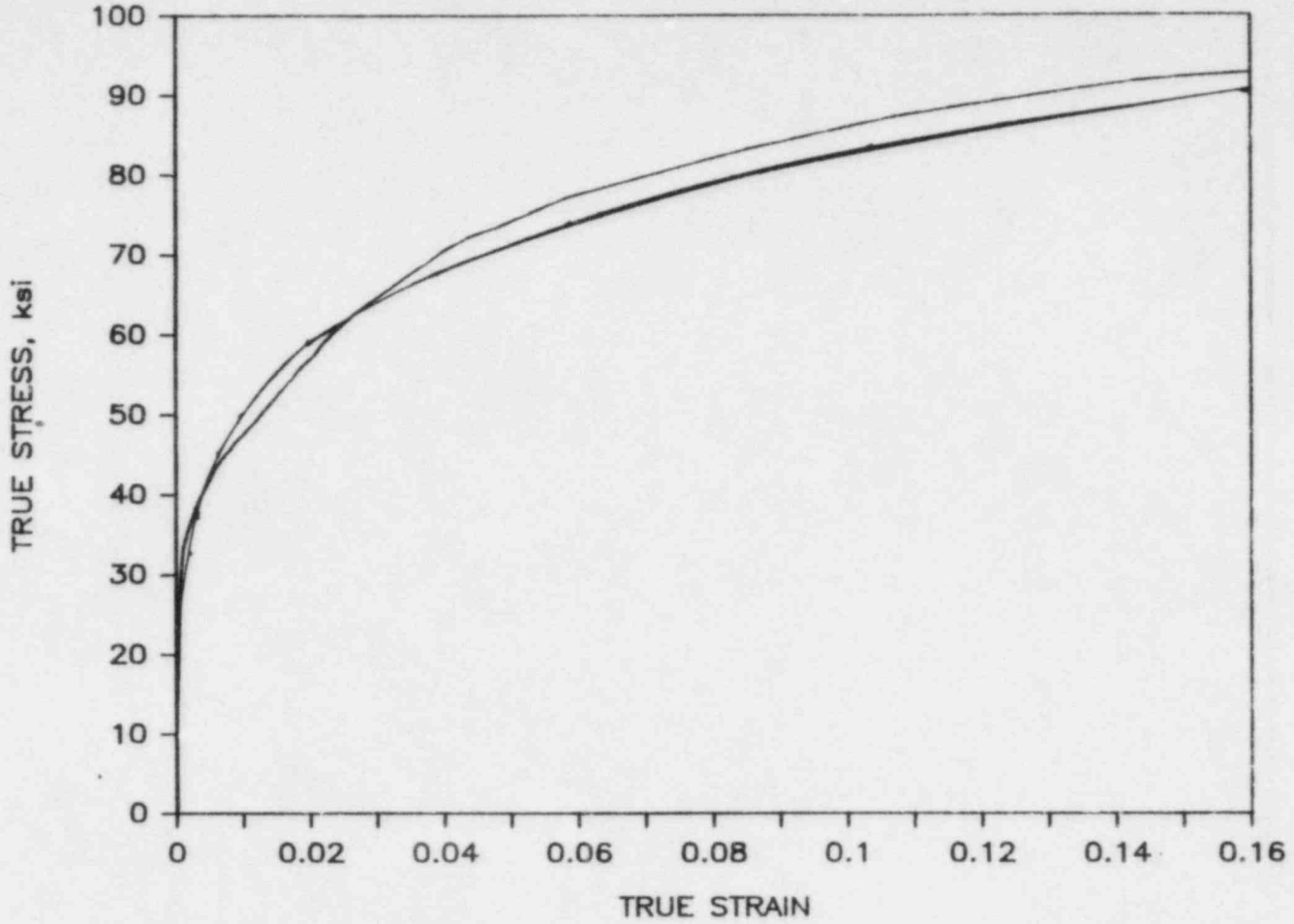

Figure 4-8. J-T Diagram for Weld Metal
(28 Inch Pipe)

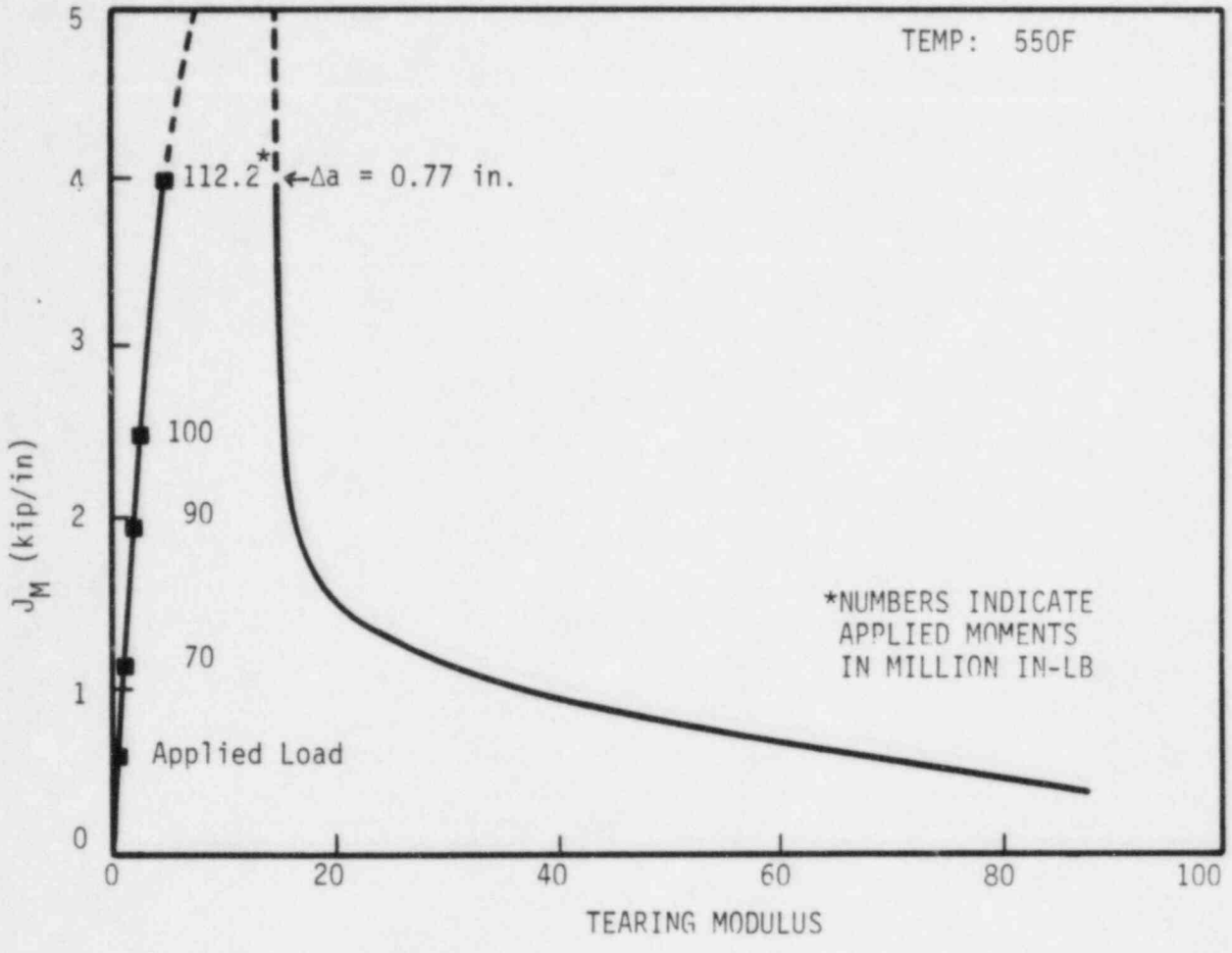

Figure 4-9. J-T Diagram for Base Metal
(28 Inch Pipe)

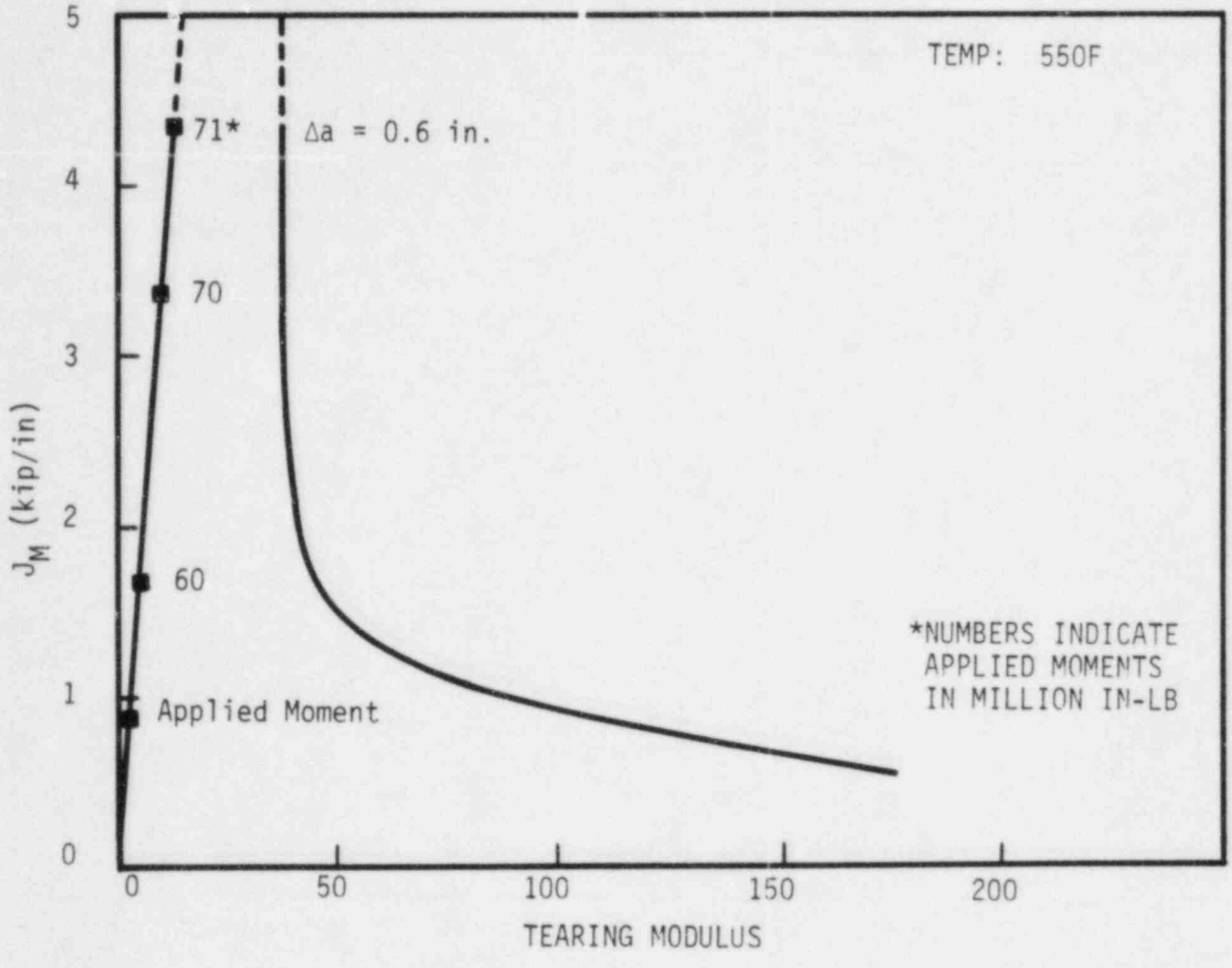

Figure 4-10. J vs. Moment Diagram for 28 Inch Pipe with Weld Metal Properties (EPRI/GE Method)

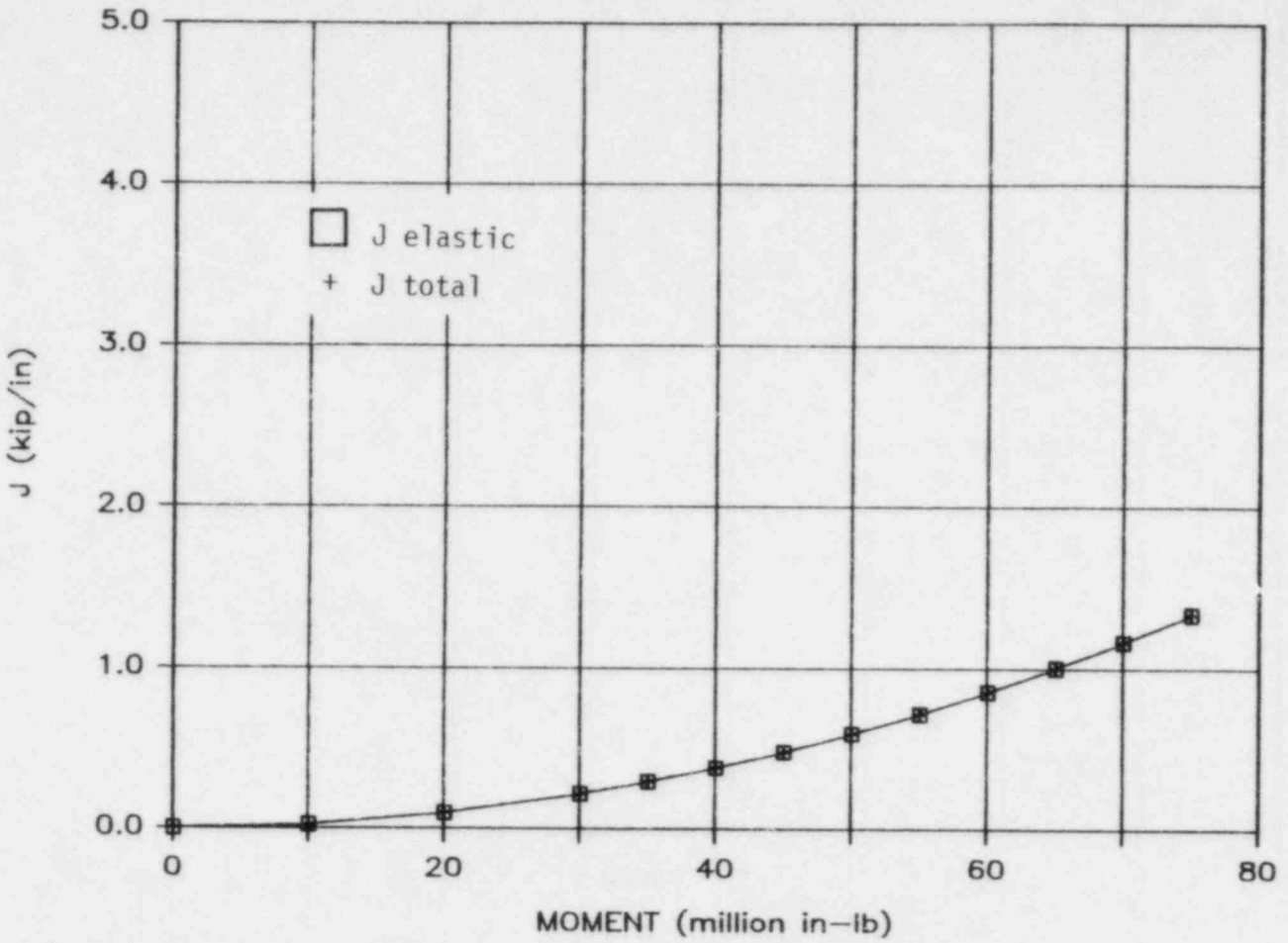

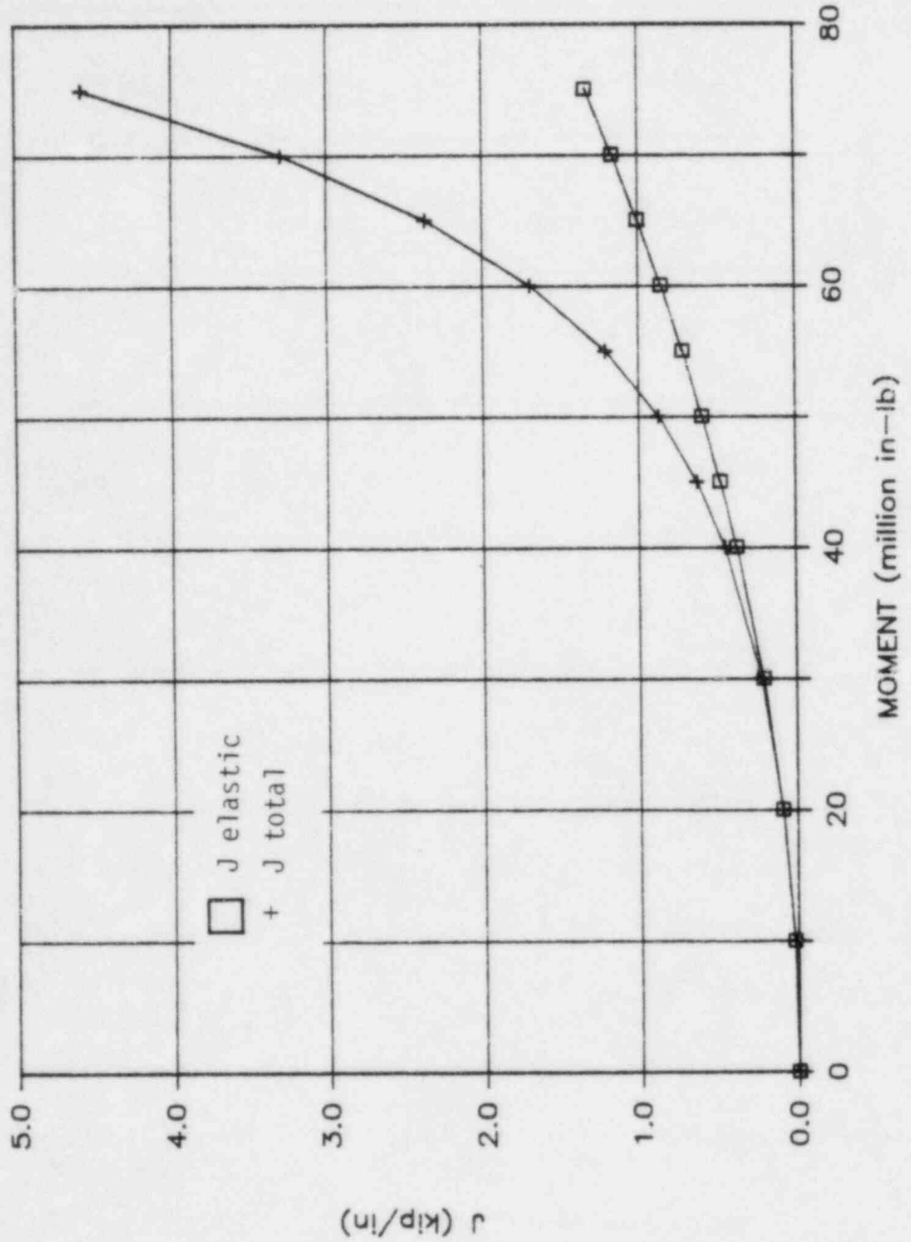

Figure 4-11. J vs. Moment Diagram for 28 Inch Pipe With Base Metal Properties (EPRI/GE Method)

Figure 4-12. J vs. Loads Diagram for 28 Inch Pipe with Base Metal Properties (Finite Element Method)

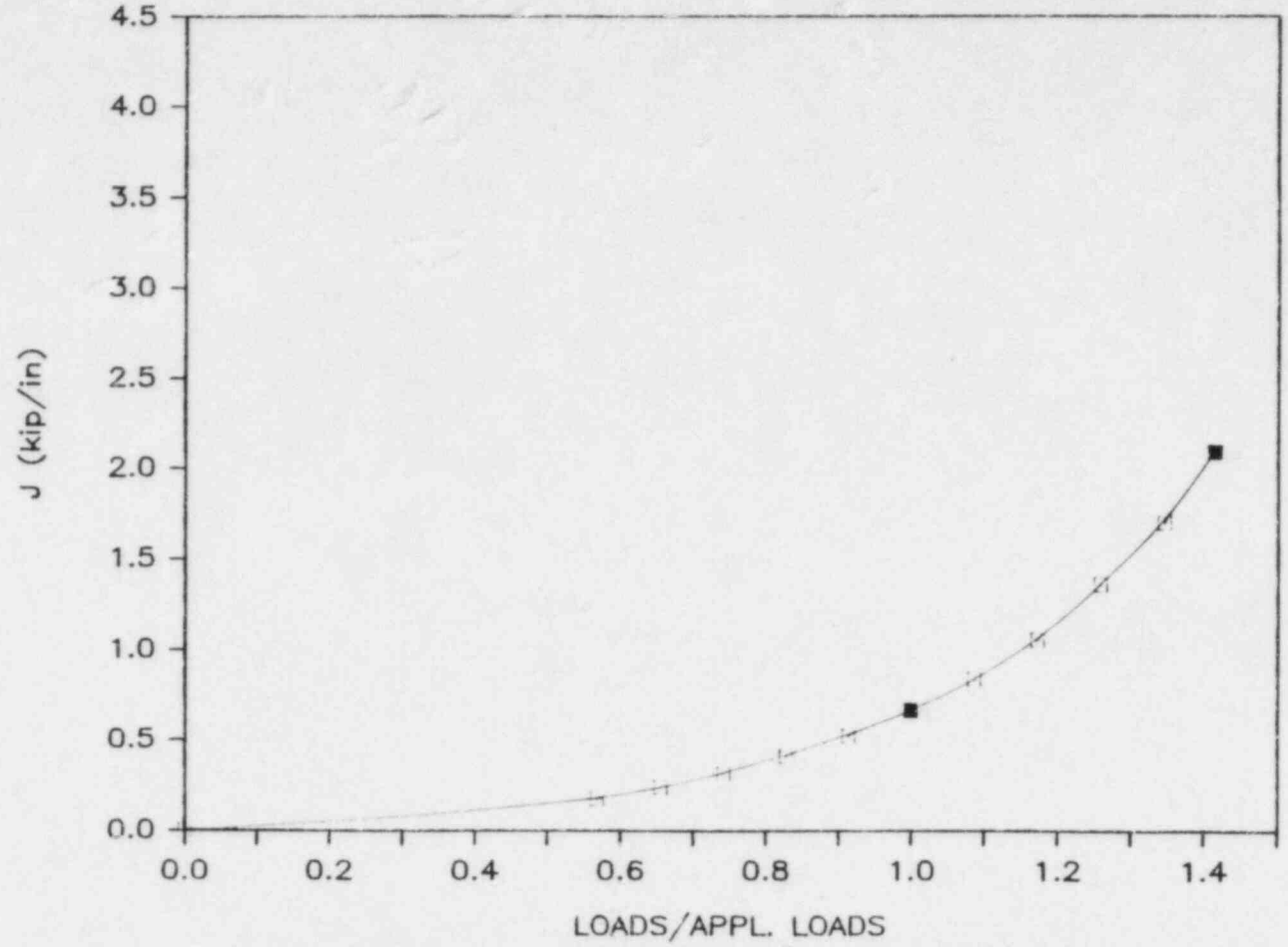

5. CONCLUSIONS

The postulated break (DEGB) required by GDC-4 is not only excessively conservative but also implausible and could reduce over-all plant safety if the passive LOCA restraint were unexpectedly impacted by piping movements due to thermal growth and/or failed snubbers exist during normal operating conditions.

This evaluation of the B&WOG plants, RCS primary piping for B&W designed NSS's has shown that postulated thru-wall flaws based on conservative detectable leakage rates result in no flaw growth when conservative bounding values of loads and material properties are used. Even if a safety factor of $\sqrt{2}$ is applied to this already conservative load set, these postulated thru-wall flaws show either no flaw growth or stable flaw growth. In addition, these postulated leakage flaw sizes are much smaller than the critical flaw size which might lead to failure of the pipe. Thus, with no known mechanism for developing a large break without going through an extended period during which the flaw would leak copiously, a controlled plant shutdown can occur before the potential exists for failure of the piping in a catastrophic manner.

6. REFERENCES

1. Letter from Harold Denton (NRC) to Murray Edelman (AIF) dated May 2, 1983.

2. Letter from J. J. Ray (ACRS) to William Dircks (NRC) dated June 14, 1983.

3. BIGIF -- Fracture Mechanics Code for Structures, User's Manual, UPGD-TM-31, Rev. A, Version 2.1A, Babcock & Wilcox, Lynchburg, Virginia, May 1984.

4. KRAKFLO -- FORTRAN Program for Calculating Flow Through Narrow Cracks, UPGD-TM-38, Babcock & Wilcox, Lynchburg, Virginia, May 1984.

5. Private communication between M. L. Boyle (USNRC) and J. R. Biller B&W, December 1983.

6. P.C. Paris and H. Tada, The Application of Fracture Proof Design Methods Using Tearing Instability Theory to Nuclear Piping Postulating Circumferential Through Wall Cracks, NUREG/CR-3464, September 1983.

7. M.E. Mayfield et al., "Cold Leg Integrity Evaluation," NUREG CR-1319, Battelle Columbus Laboratories, 2/80.

8. D. Abhollahan and B. Chexal, "Calculation of Leak Rates Through Cracks in Pipes and Tubes," EPRI-NP-3395, 1983.

9. MARC -- General Purpose Finite Element Program User Manual, MARC Analysis Research Corp., Palo Alto, California.

10. J.C. Nagtegaal, "Finite Element Analysis of Fracture Mechanics Problems," MARC Analysis Research Corp., Palo Alto, CA.

11. R.S. Barsoum, "One the Use of Isoparametric Finite Elements in Linear Elastic Fracture Mechanics, "International Journal on Numerical Methods in Engineering, Vol. 9, 1975, pp. 495-507.

12. Parks, D. M., "A Stiffness Derivative Finite Element Technique for Determination of Elastic Crack Tip Stress Intensity Factors, " International Journal of Fracture Mechanics, Vol. 10, No. 4, December, 1974.

13. J. Rice, "A Path Independent Integral and the Approximate Analysis of Strain Concentration by Notches and Cracks," Journal of Applied Mechanics, June 1968, pp. 379-386.

14. V. Kumar, et al. "Advances in Elastic-Plastic Fracture Analysis," EPRI NP-3607, August 1984.

15. P. Paris, Appendix B, NUREG-0744, Vol. 1, Rev. 1, July 1982.

16. Handout at NRC/AIF Load Combination Subcommittee Meeting, Gaithersburg, Md., Oct. 25, 1983.

17. BAW-1889P, "Piping Material Properties for Leak-Before-Break Analysis," B&W Proprietary Report, September 1985.

18. NUREG-1061, Vol. 3, "Report of the U.S. NRC Piping Review Committee - Evaluation of Potential for Pipe Breaks," U.S. Nuclear Regulatory Commission, Nov. 1984.

19. G. M. Wikowski et al., "Degraded Piping Program - Phase II, Semi-annual Report (Oct. 84 - Mar. 85)," NUREG/CR-4082, Vol. 2., Battelle's Columbus Laboratories, July 1985.